EUFAR 2nd Summer School on
Airborne Cloud and Aerosol Science

Aerosol Optical Properties

by

Andreas Petzold

Institut für Physik der Atmosphäre
Deutsches Zentrum für Luft- und Raumfahrt
Oberpfaffenhofen
82234 Wessling

andreas.petzold@dlr.de

Aerosol-Climate Interaction

direct effect

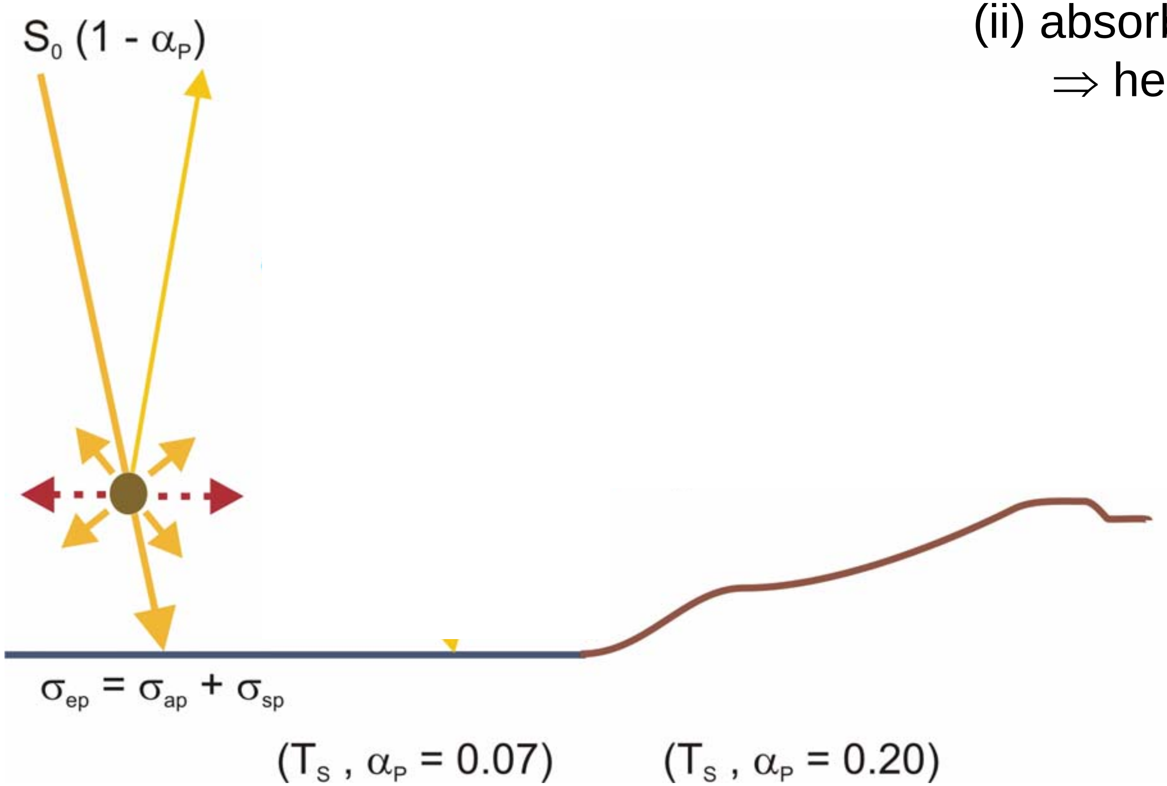

Direct effect

resulting from interaction with airborne particles solar radiation is

(i) scattered back into space
⇒ cooling effect,

(ii) absorbed in the atmosphere
⇒ heating effect.

Aerosol-Climate Interaction

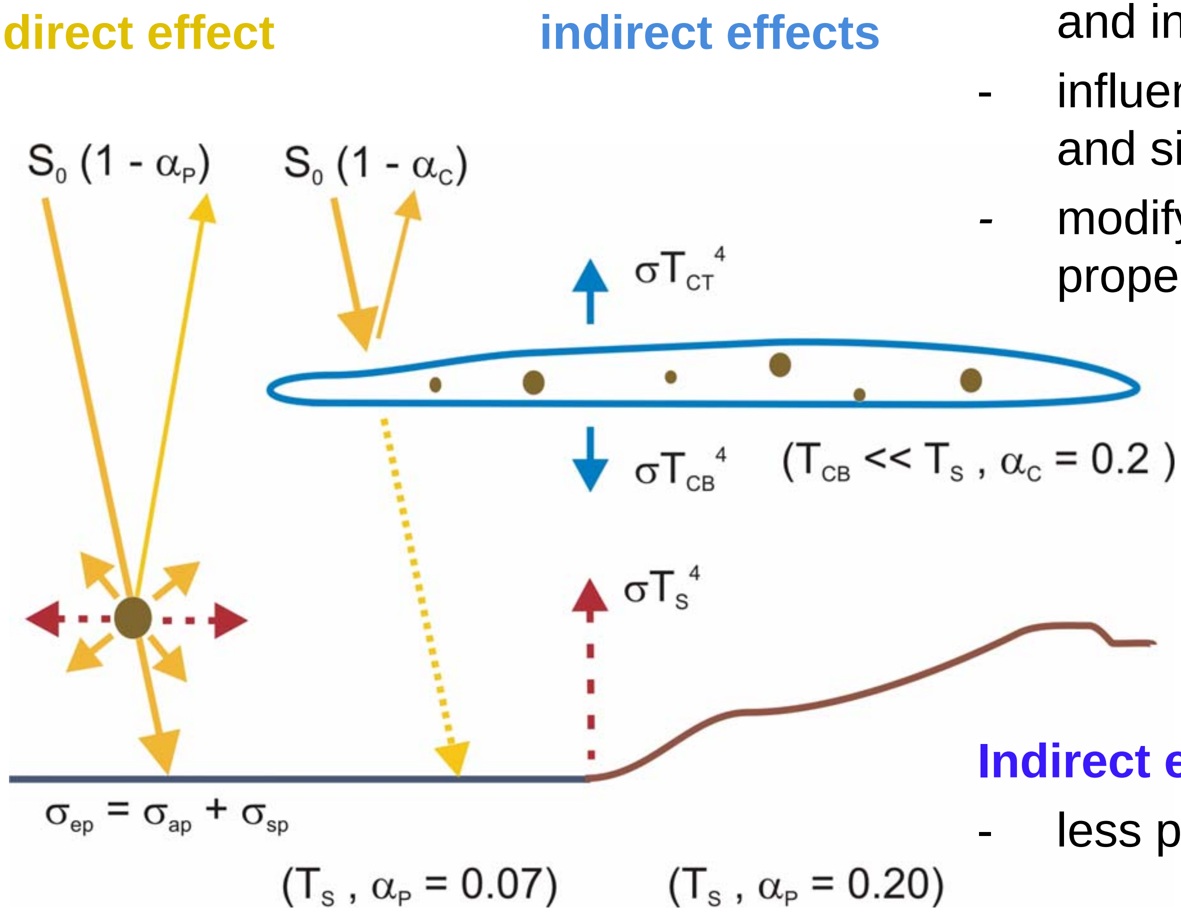

Indirect effects (warm clouds)

aerosol particles

- act as cloud condensation nuclei and initiate cloud formation;
- influence number concentration and size of cloud elements;
- modify life cycle and radiative properties of clouds.

Indirect effects (ice clouds)

- less pronounced, still unclear.

Aerosol-Climate Interaction

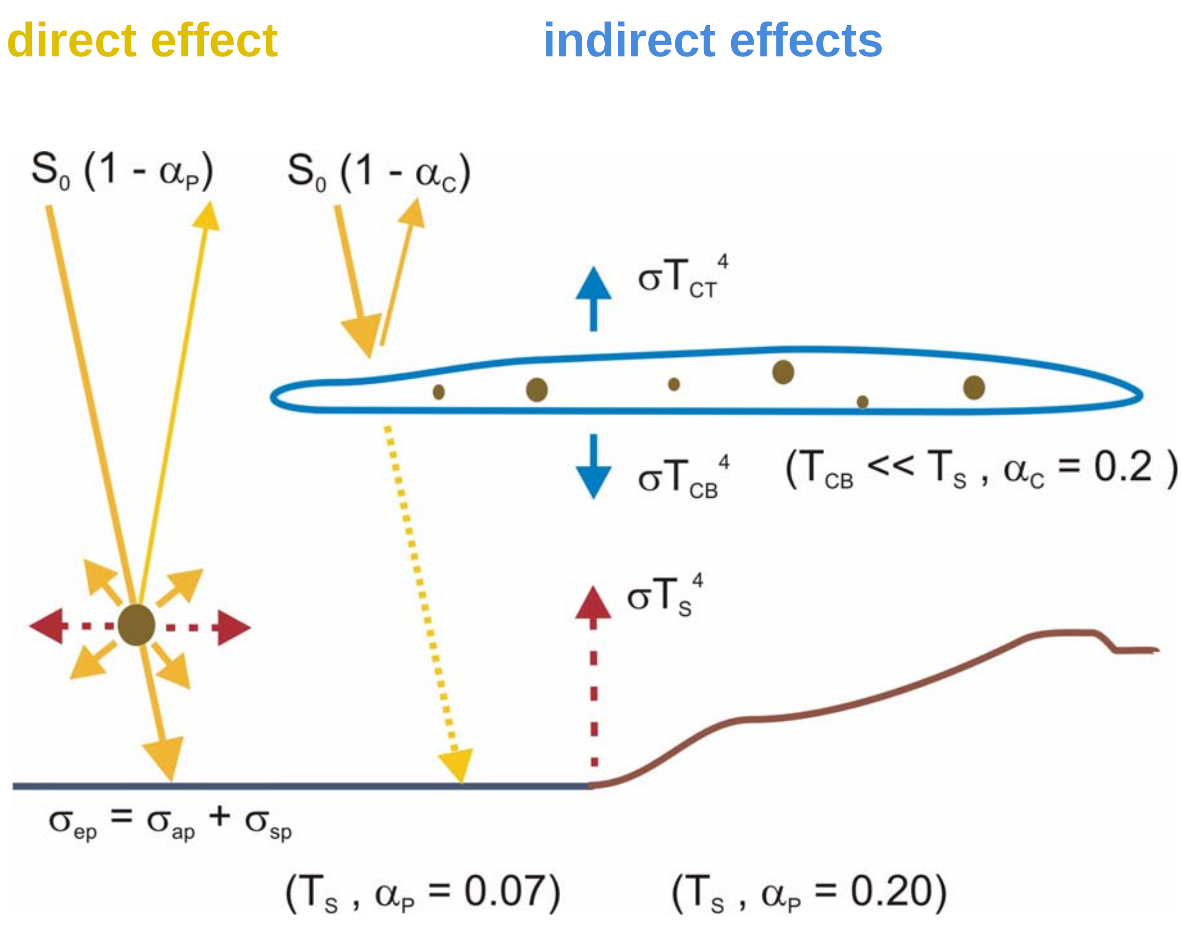

α = surface reflectivity or albedo

σ = coefficient of
extinction (ep)
absorption (ap)
scattering (sp)
in 1 / km

AOT = aerosol-optical thickness
$$= \int \sigma_{ep}(z)\ dz$$

SSA = single-scattering albedo (ω_0)
$$= \sigma_{sp} / \sigma_{ep}$$

Angström-exponent
$$\sigma_{ep} \propto \lambda^{-å}$$

Aerosol Radiative Forcing

$$R_{SUM} = R_{BL} + R_S T_{BL}^2 (1 - R_S R_{BL})^{-1}$$

$$R_{BL} = \delta \omega_0 \bar{\beta}$$

= hemispheric backscatter

$$T_{BL} = 1 - \delta (1 - \omega_0) - \delta \omega_0 \bar{\beta}$$

= 1 - absorption - backscatter

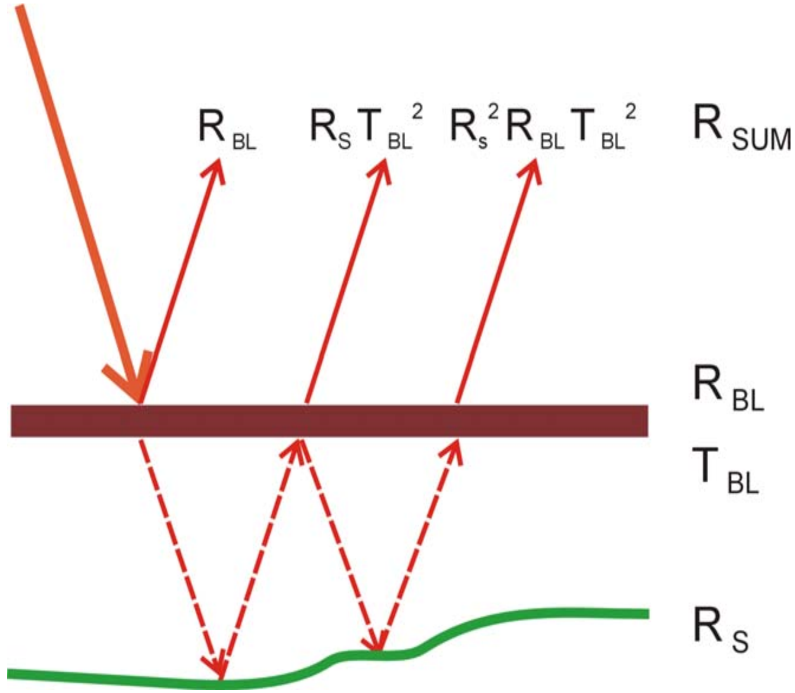

$$\Delta R = R_{SUM} - R_S \cong \delta \omega_0 \bar{\beta} \times \{ (1 - R_S)^2 - 2 R_S \bar{\beta}^{-1} (\omega_0^{-1} - 1) \}$$

particle optical properties relevant for climate interaction:

aerosol optical thickness δ
hemispheric backscatter fraction
single-scattering albedo

Köpke, 1992

Global Aerosol Distribution from Spaceborne Observation

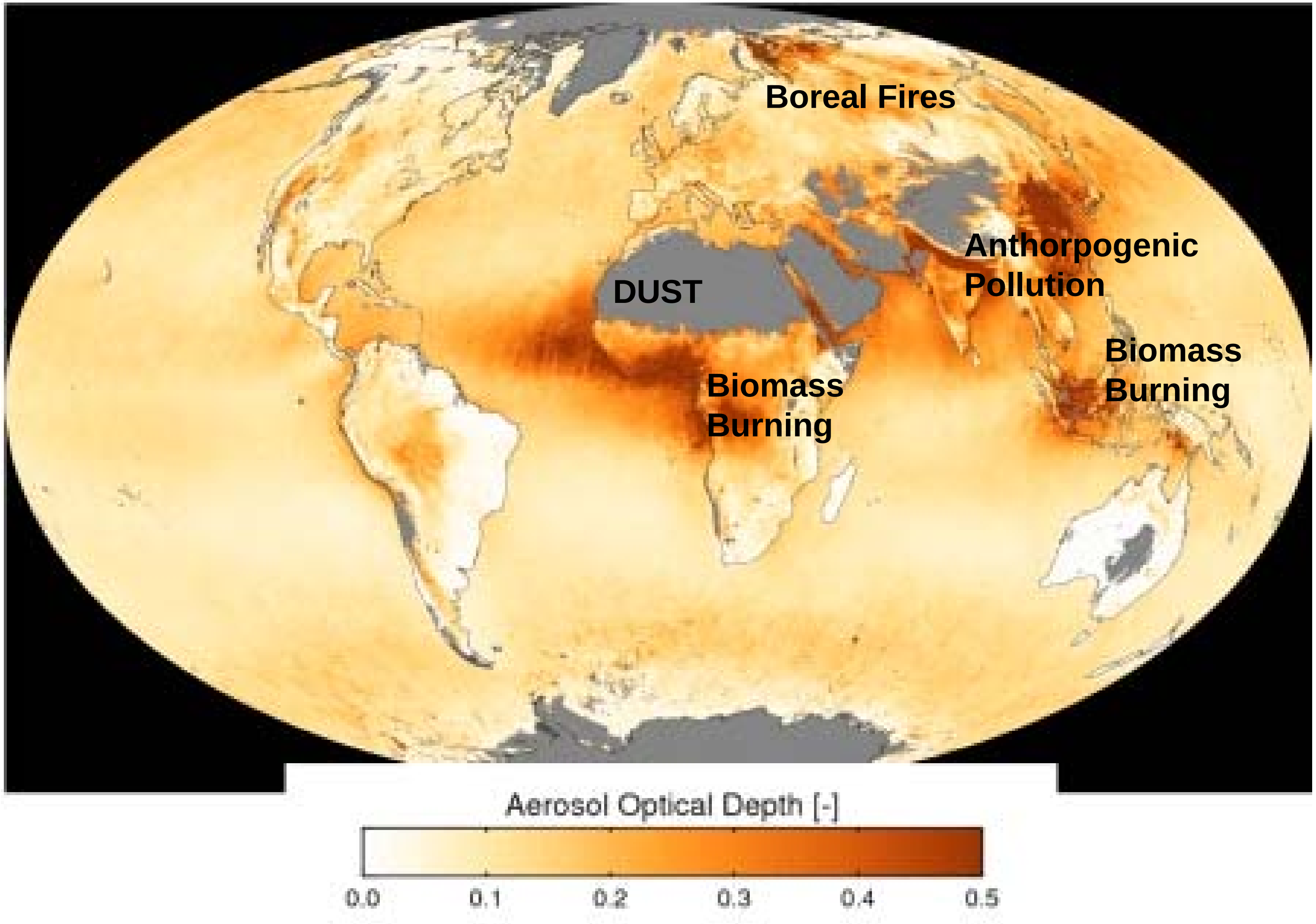

http://climate.gsfc.nasa.gov/viewImage.php?id=199
Image of the Week - February 18, 2007

Aerosol Optical Properties are Relevant for ...

Aerosol-Climate Interaction

The impact of aerosol particles on Earth's climate is based on the interaction of particles and hydrometeors (cloud droplets, ice crystals, ...) with visible (solar) and infrared (terrestrial) radiation.

Remote Sensing of Atmospheric Aerosol

The remote sensing of aerosol particles from ground or space by passive (sun photometer, spectro-radiometer) or active (LIDAR) methods is based on the interaction of particles with electromagnetic radiation. Aerosol optical thickness is defined as the integral over the aerosol extinction coefficient.

Size Measurement of Aerosol Particles

The majority of particle sizing methods particularly for the particle diameter size range > 100 nm are based on light scattering methods.

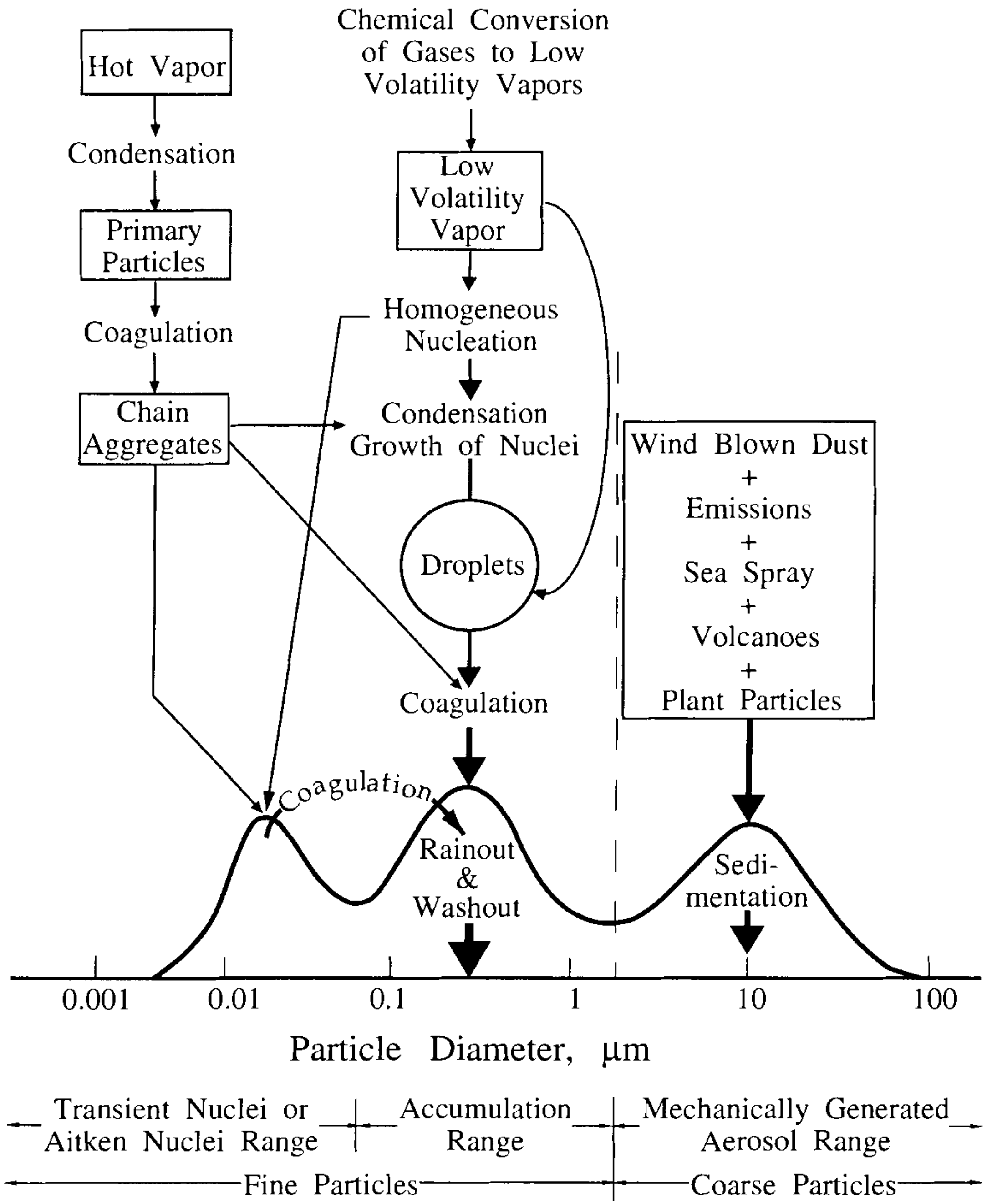

Seinfeld and Pandis
Atmospheric Chemistry
and Physics, 1998

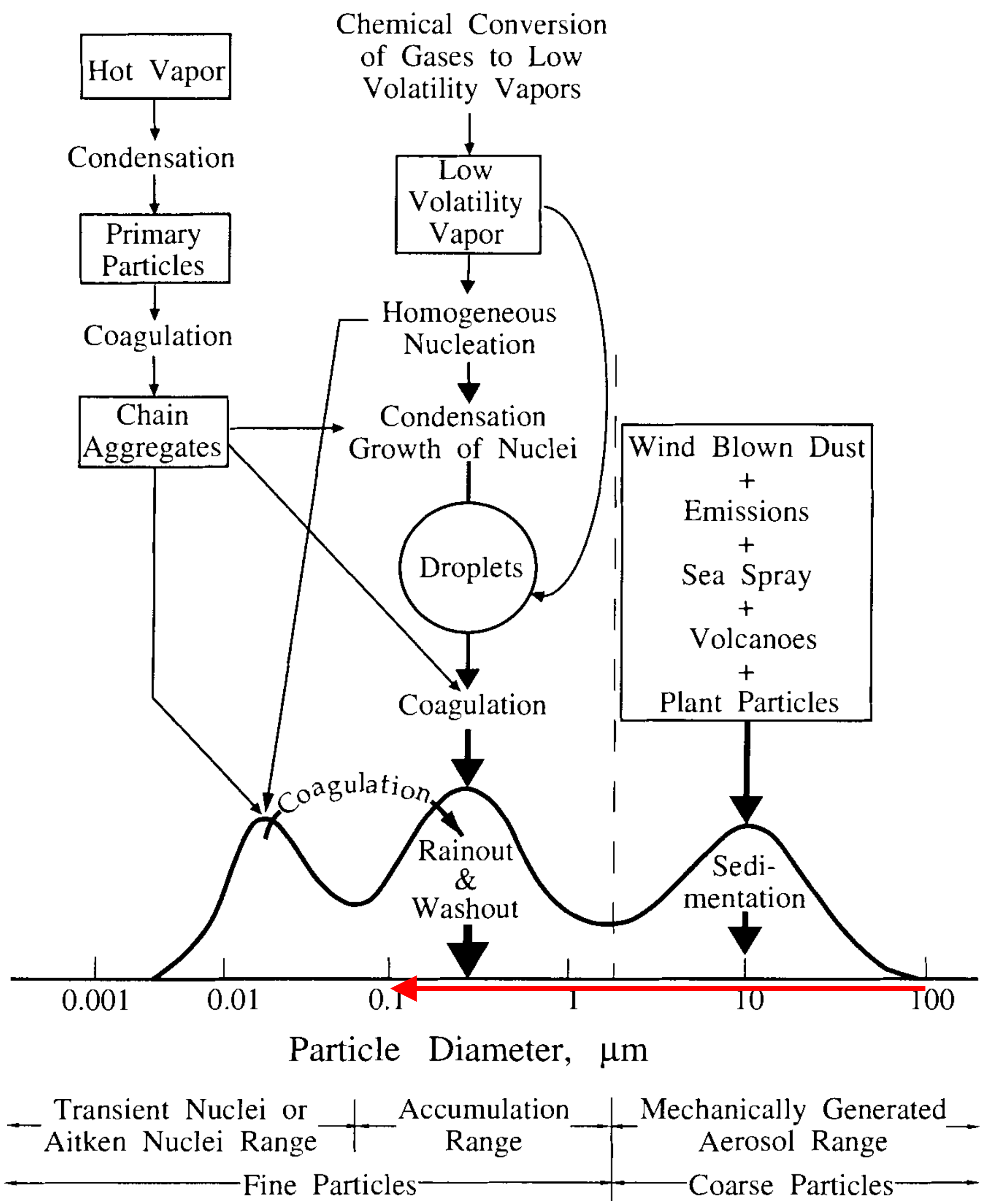

size range of optically active particles for visible light

Seinfeld and Pandis
Atmospheric Chemistry and Physics, 1998

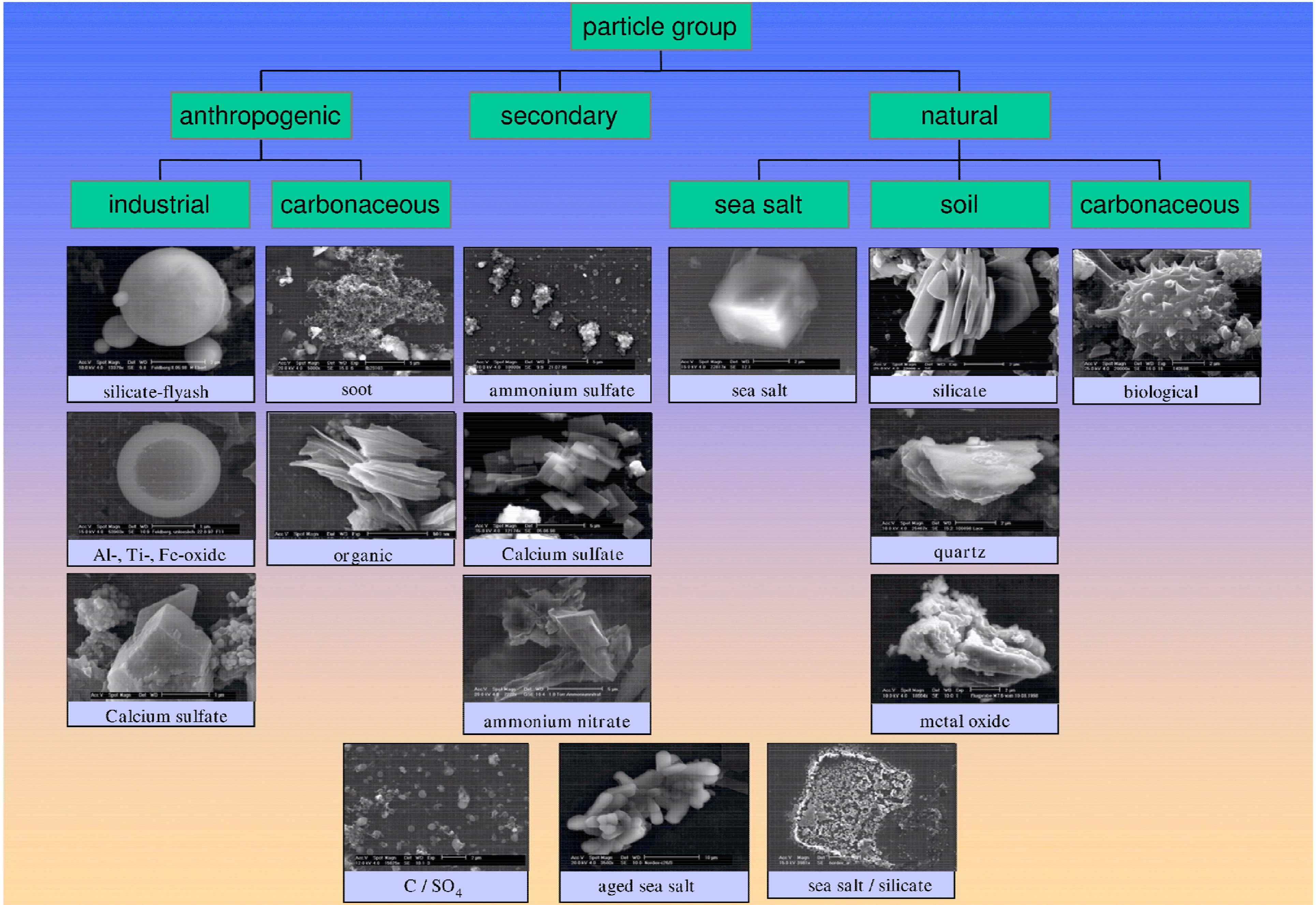
particle group
anthropogenic
secondary
natural
industrial
carbonaceous
sea salt
soil
carbonaceous
silicate-flyash
soot
ammonium sulfate
sea salt
silicate
biological
Al-, Ti-, Fe-oxide
organic
Calcium sulfate
quartz
Calcium sulfate
ammonium nitrate
metal oxide
C / SO4
aged sea salt
sea salt / silicate

Direct Climate Effect of Anthropogenic Aerosol

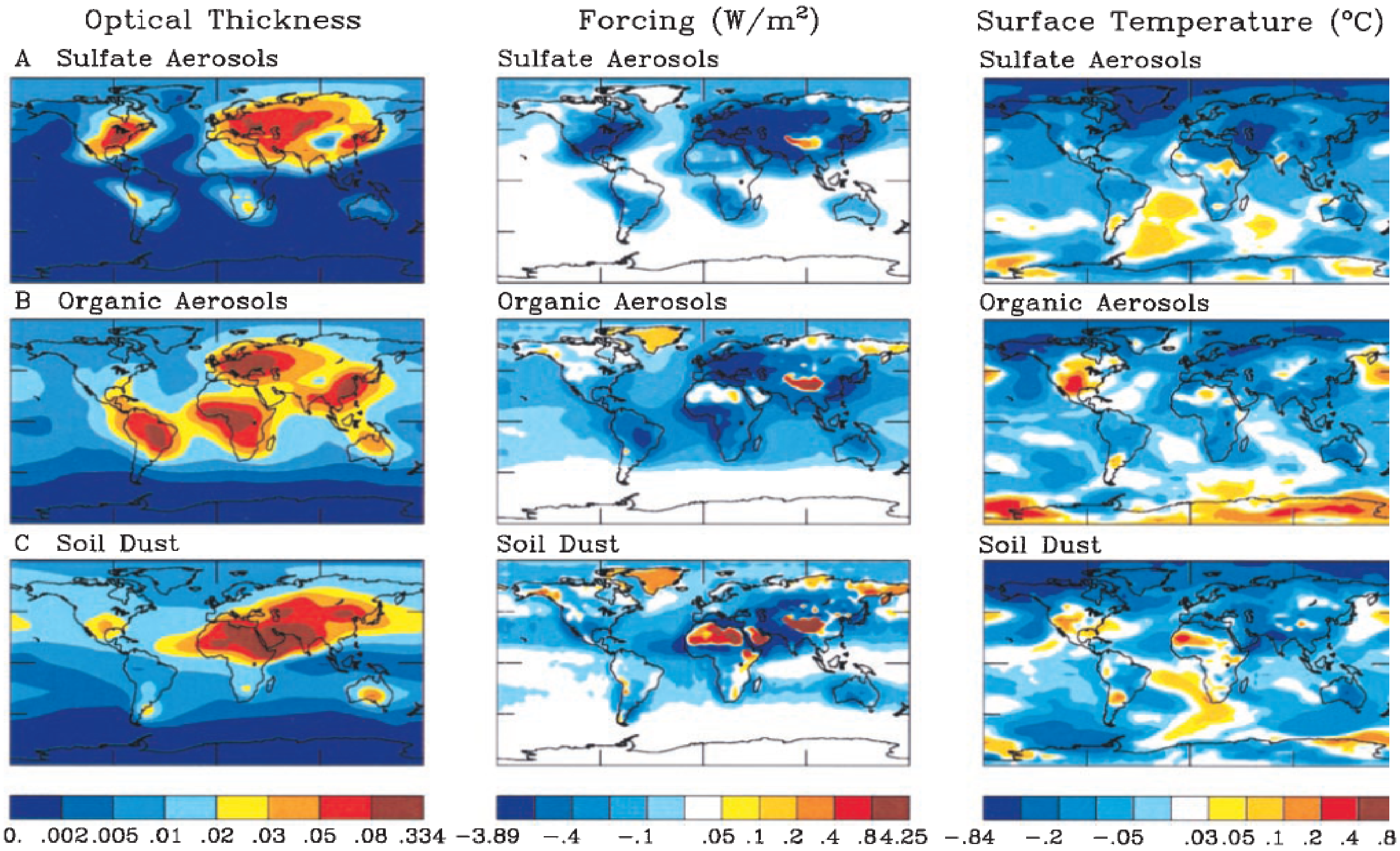

Hansen et al, Proc. Nat. Acad. Sci. 95, 12753 - 12758.

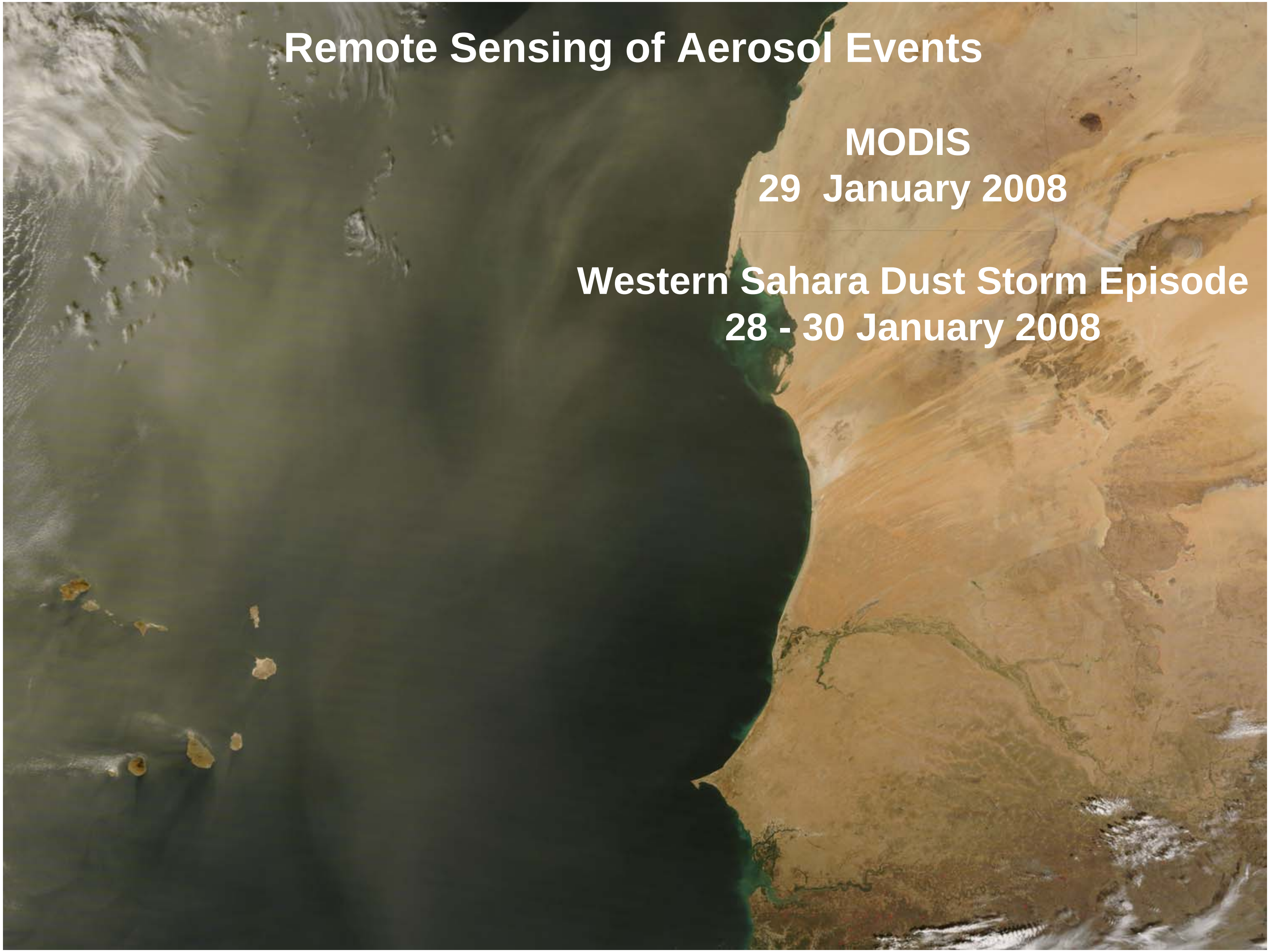
Remote Sensing of Aerosol Events
MODIS
29 January 2008
Western Sahara Dust Storm Episode
28 - 30 January 2008

Meteosat 2nd Generation 28 January 2008

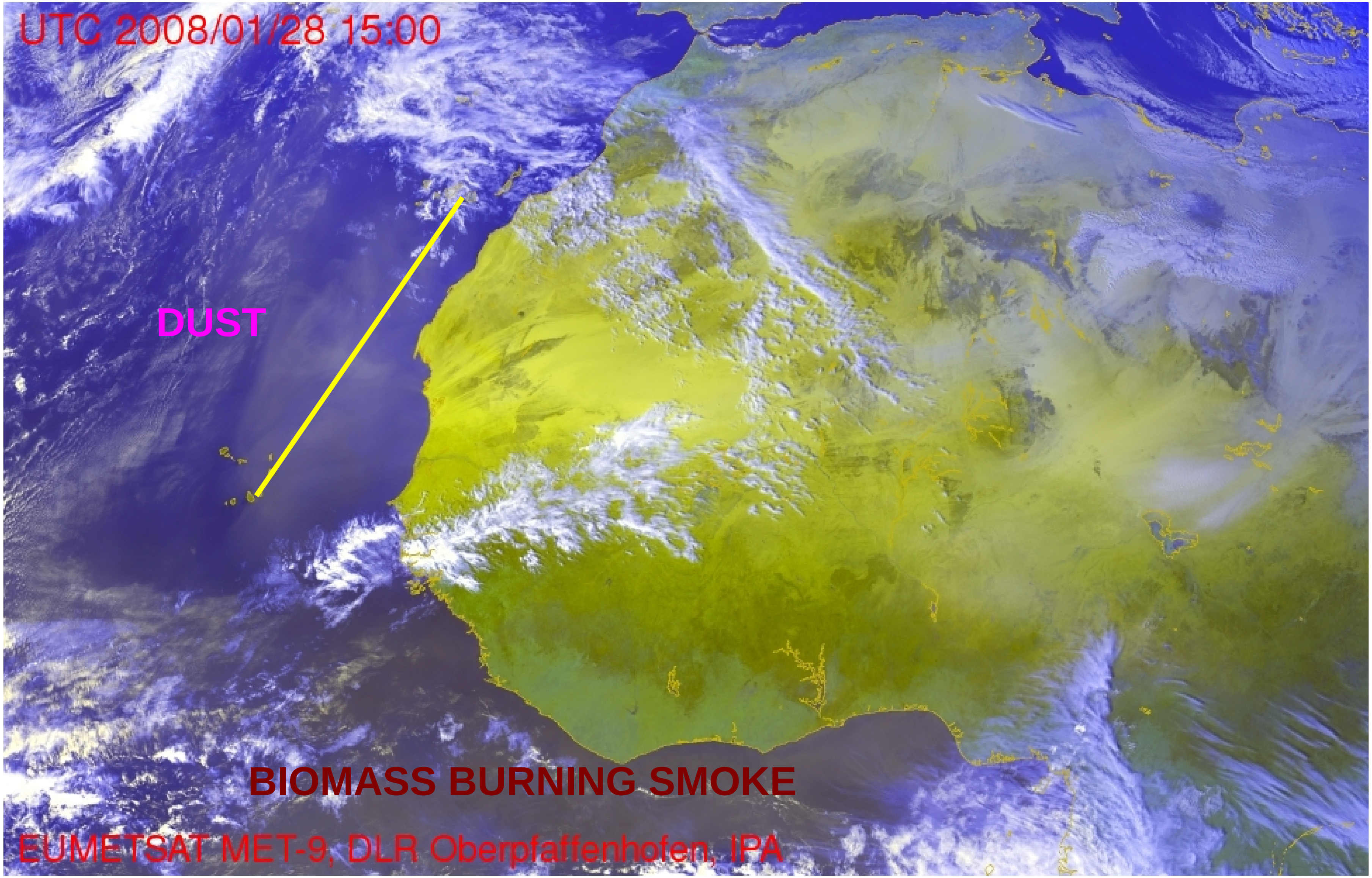

Meteosat 2nd Generation 28 January 2008

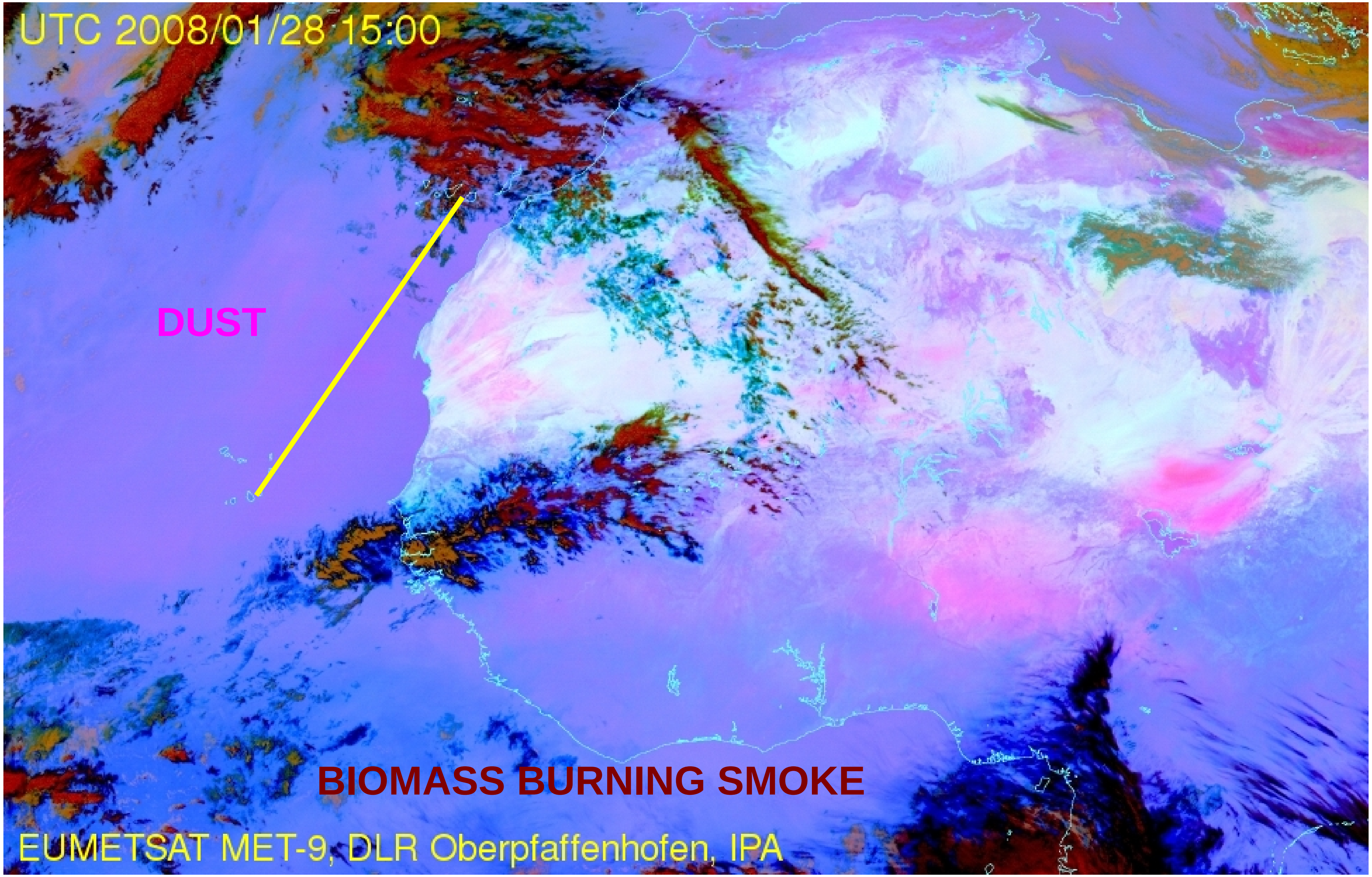

Transport of Atmospheric Aerosol - Dust

Dust layer topped by clouds at 6000 m a.s.l.

MODIS Aerosol Optical Depth 22 January 2008

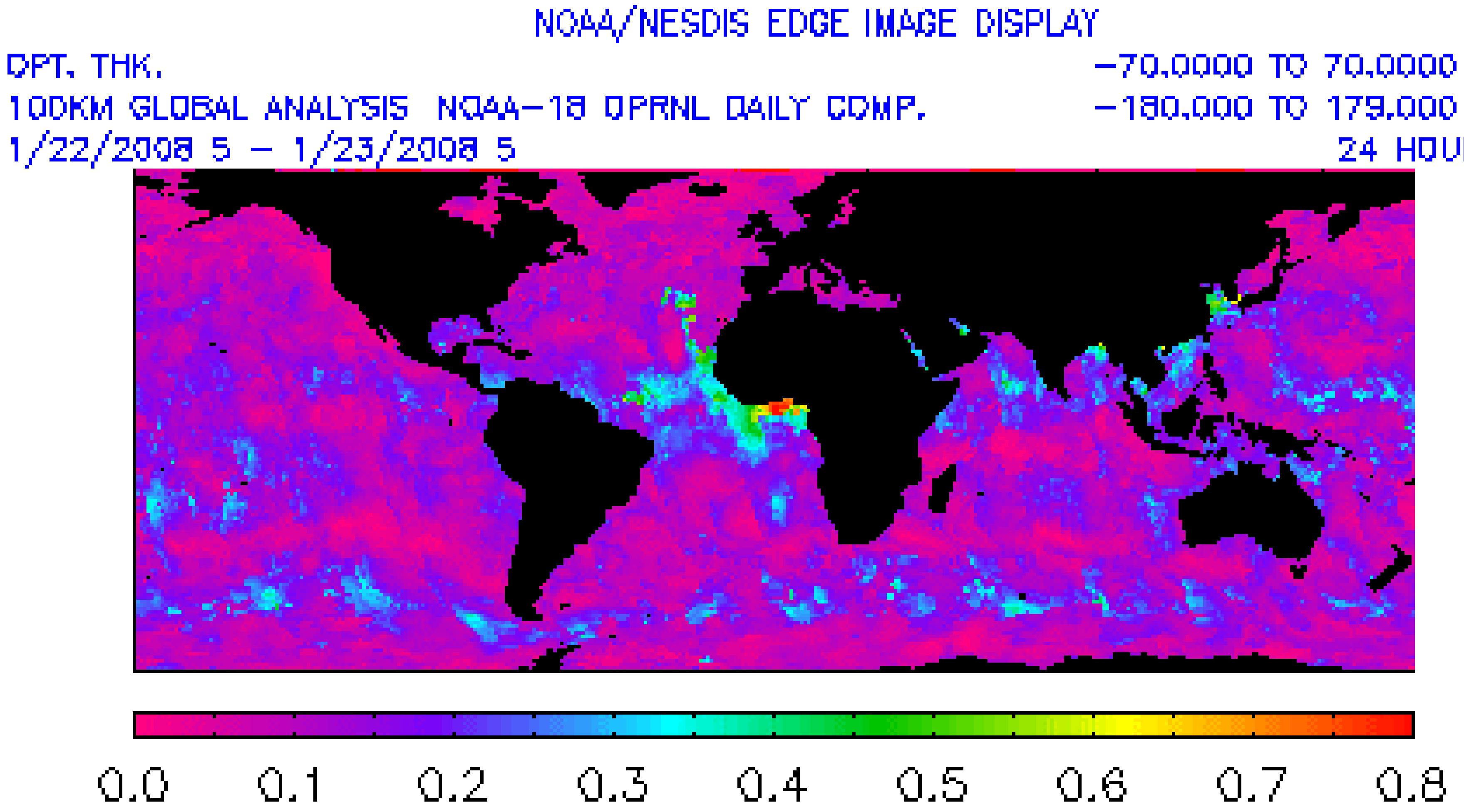

MODIS Aerosol Optical Depth 25 January 2008

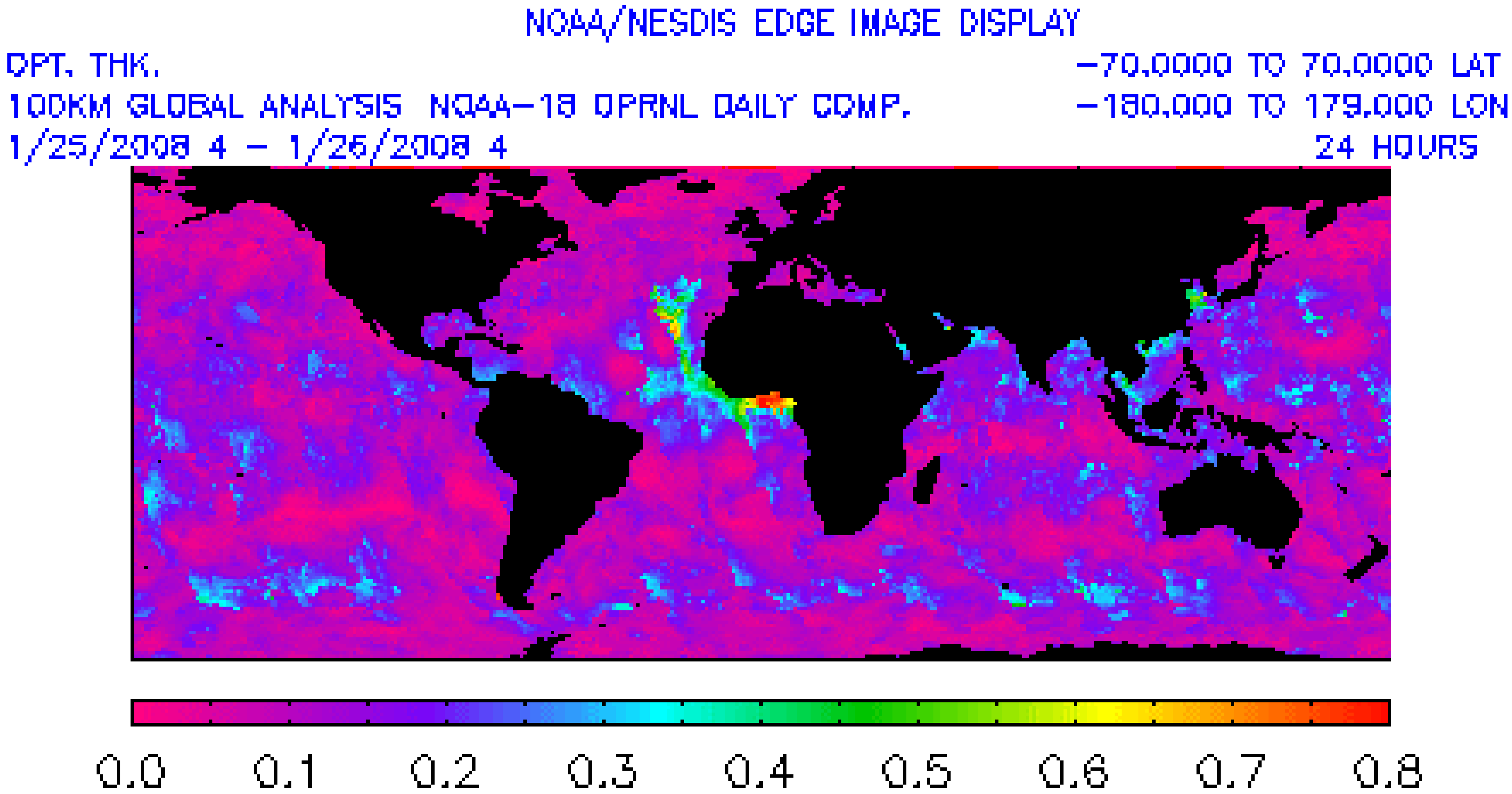

MODIS Aerosol Optical Depth 28 January 2008

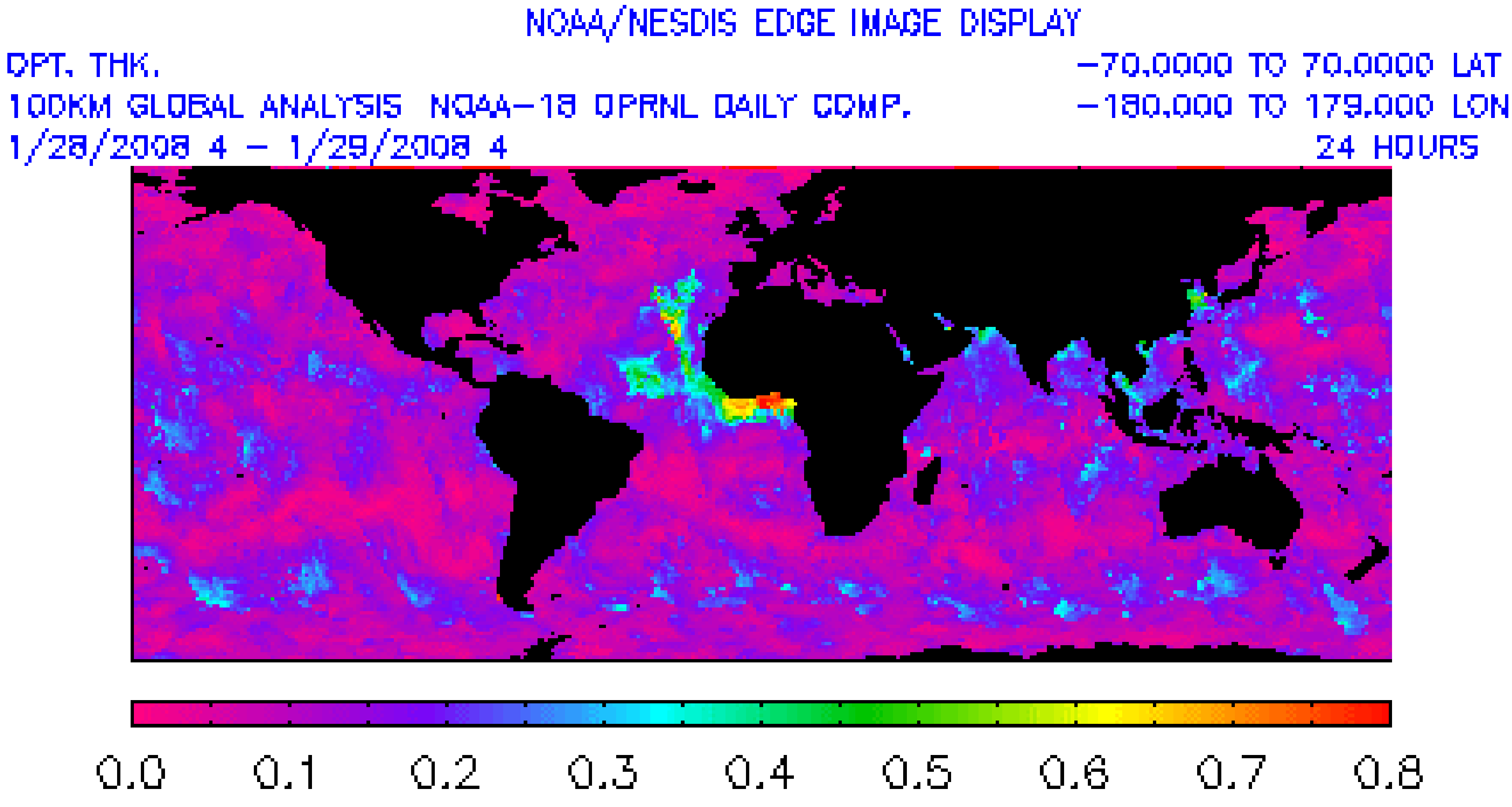

MODIS Aerosol Optical Depth 29 January 2008

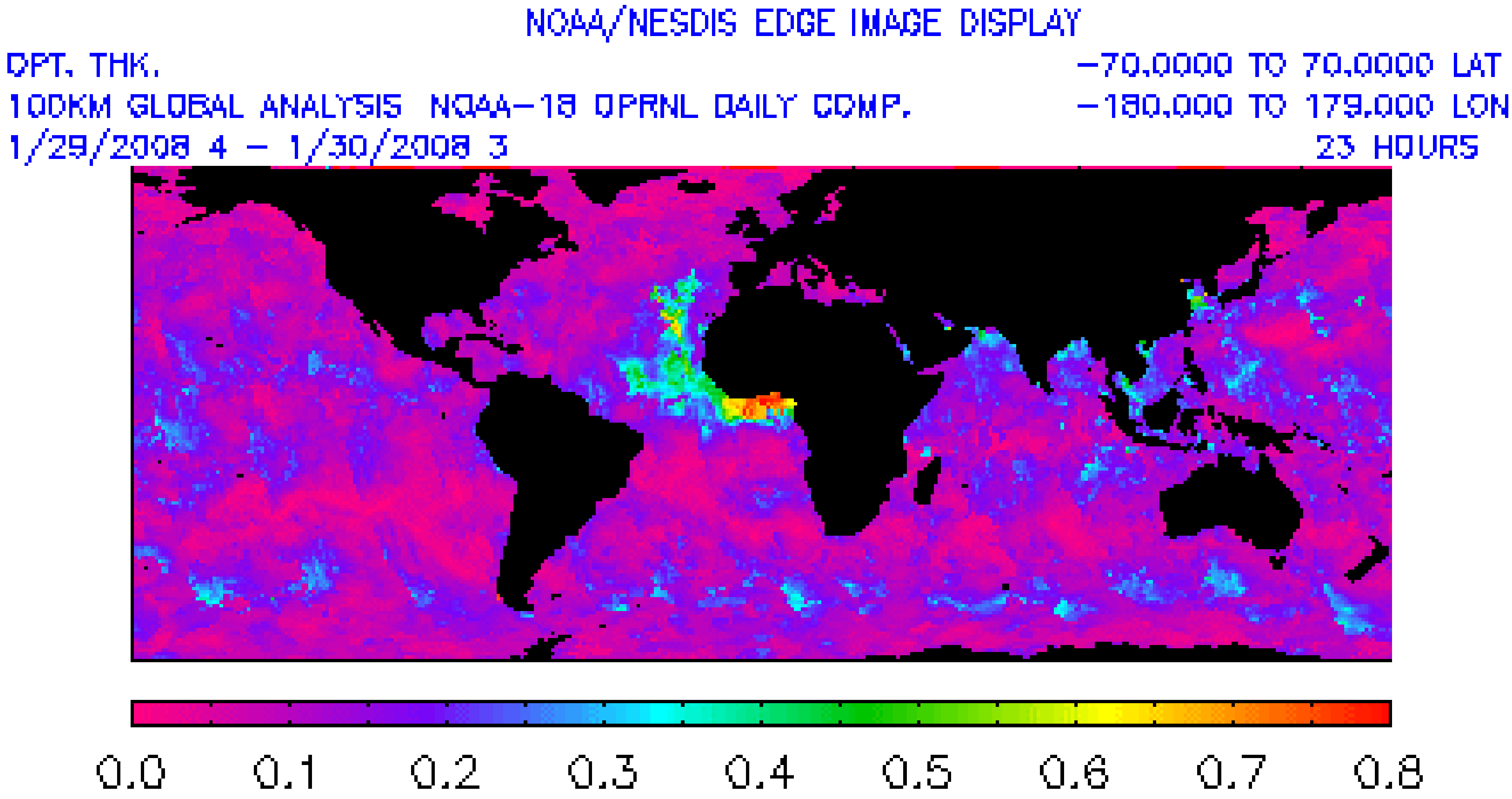

MODIS Aerosol Optical Depth 31 January 2008

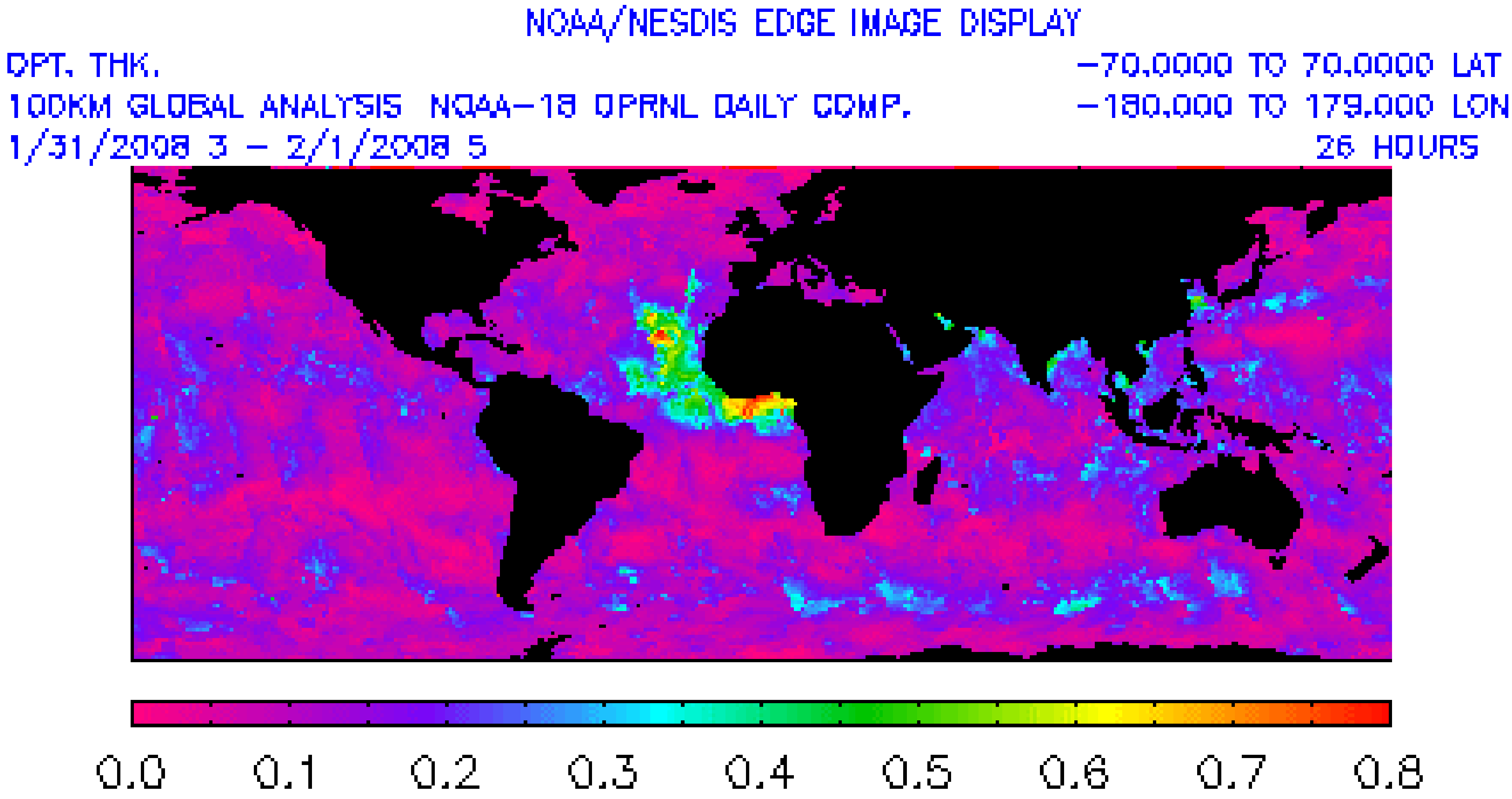

MODIS Aerosol Optical Depth 02 February 2008

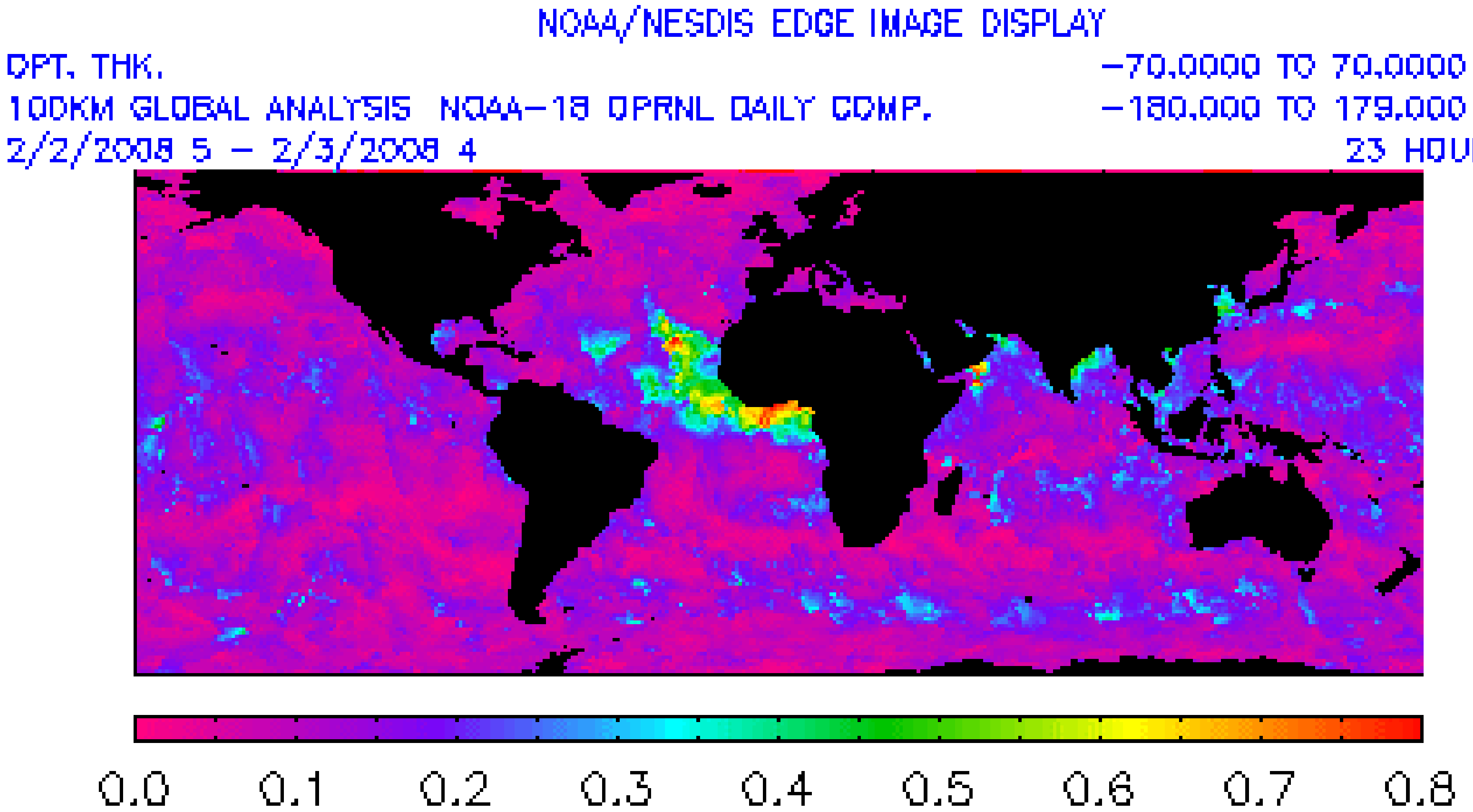

MODIS Aerosol Optical Depth 04 February 2008

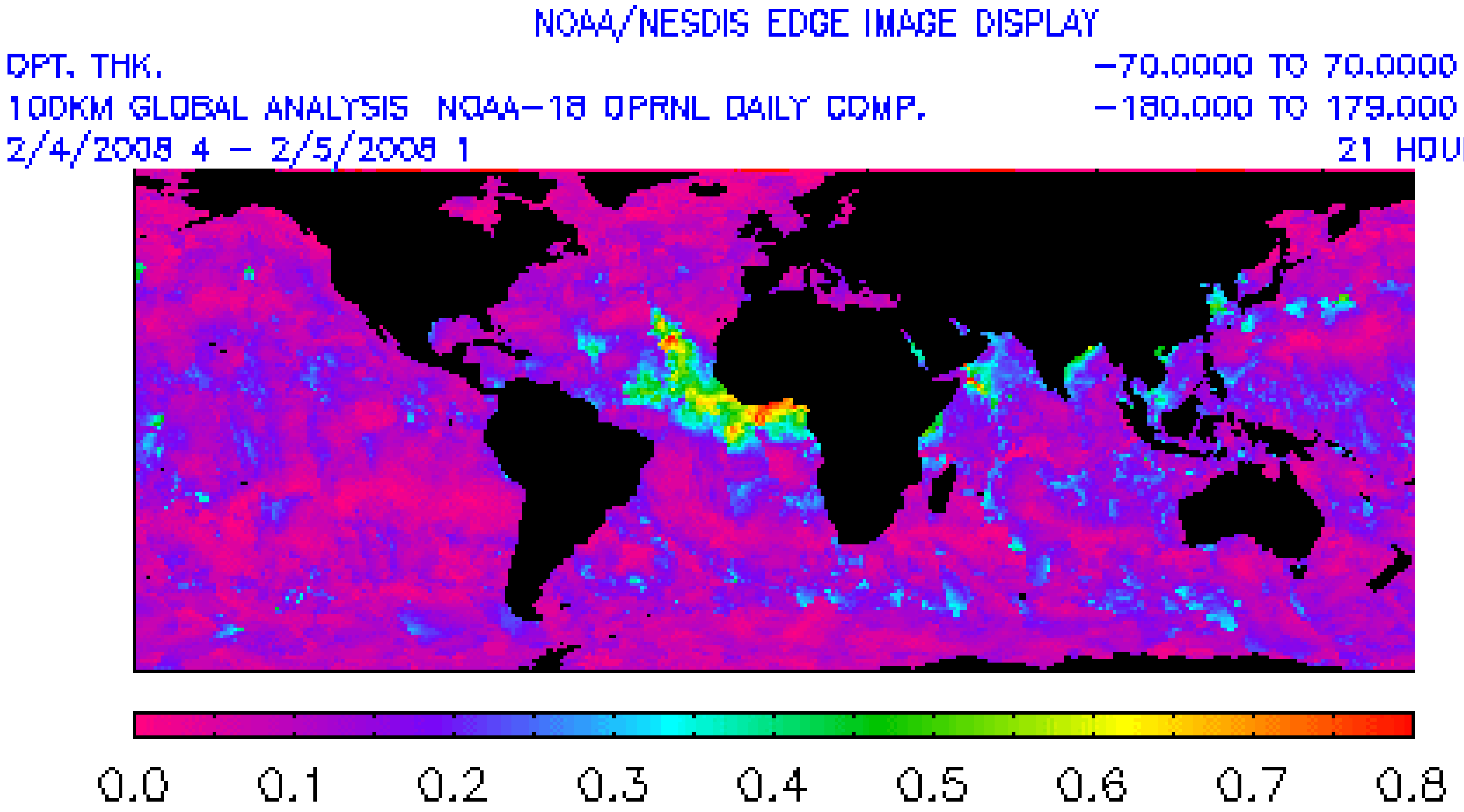

MODIS Aerosol Optical Depth 05 February 2008

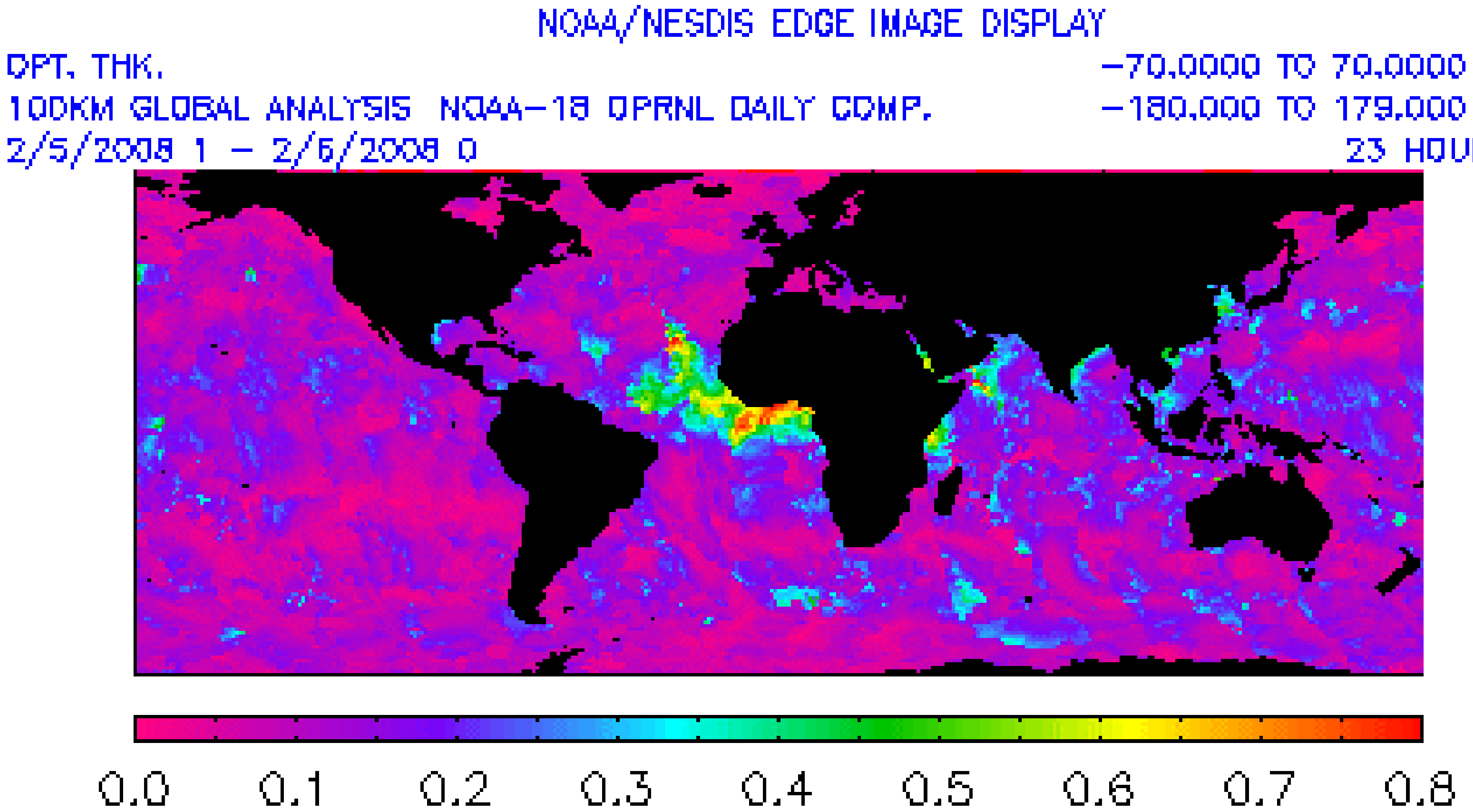

MODIS Aerosol Optical Depth 06 February 2008

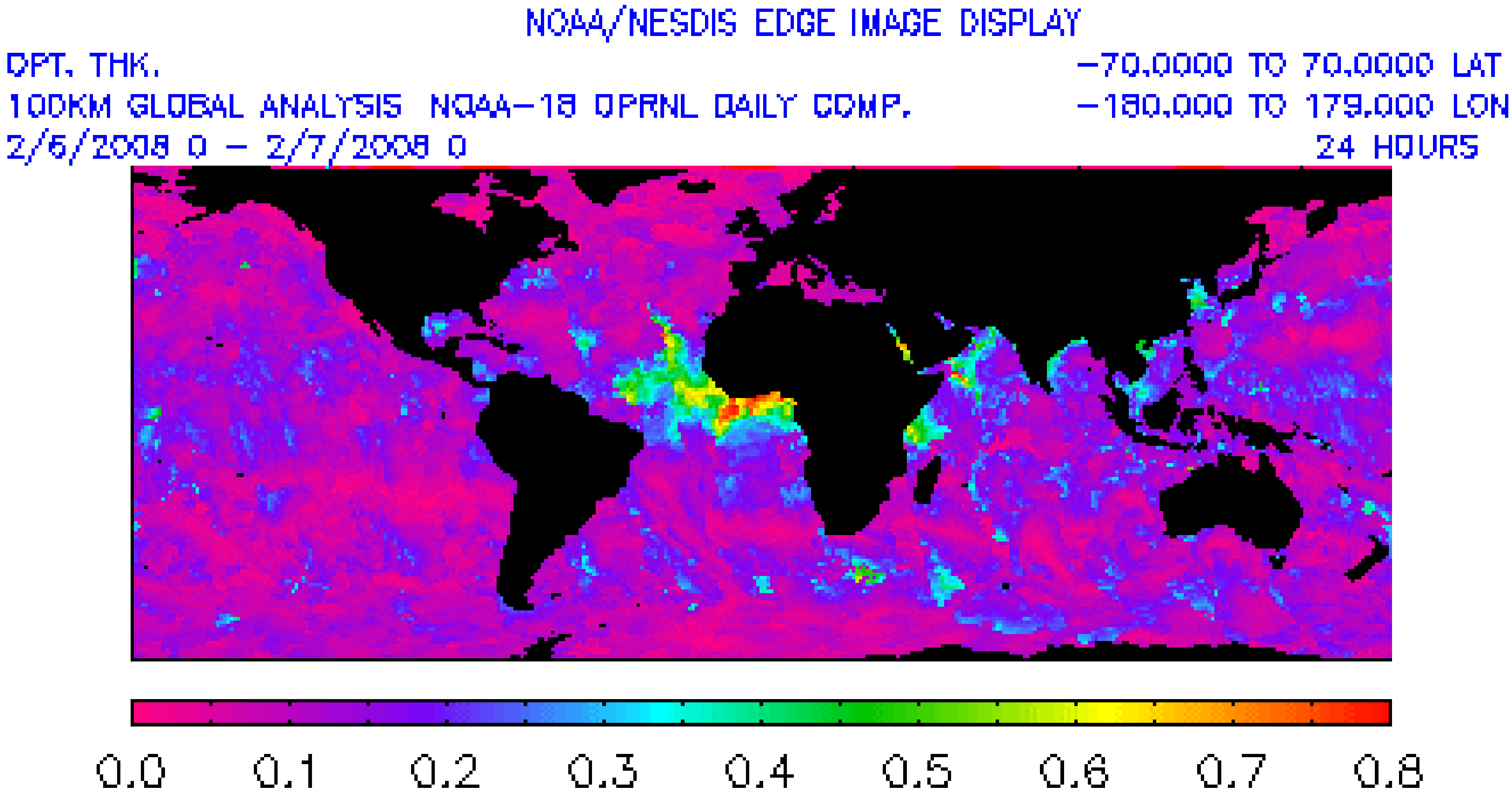

Aerosol Optical Properties

The interaction of aerosol particles with electromagnetic radiation gives rise to many spectacular atmospheric effects, such as coloured sunsets, halos around the sun or moon, and rainbows.

The aerosol impact on climate as well as visibility degradation in an aerosol-loaded atmosphere is related to the aerosol-radiation interaction.

The predominant fraction of direct-reading real-time aerosol measurement methods uses by some means or other optical detection methods.

The measurement of particle sizes for accumulation mode particles, soil and dust particles as well as for cloud drops and ice crystals is entirely based on optical methods.

Remote sensing methods for aerosols (lidar, satellite-borne radiation spectrometers) rely on the interaction of radiation and particles.

The aerosol-radiation interaction is an efficient method for transferring heat to particles which can then be used for

- particle charging by UV radiation
- particle evaporation for chemical analytical purposes
- measuring combustion particles in flames from incandescence radiation
- ...

Light extinction

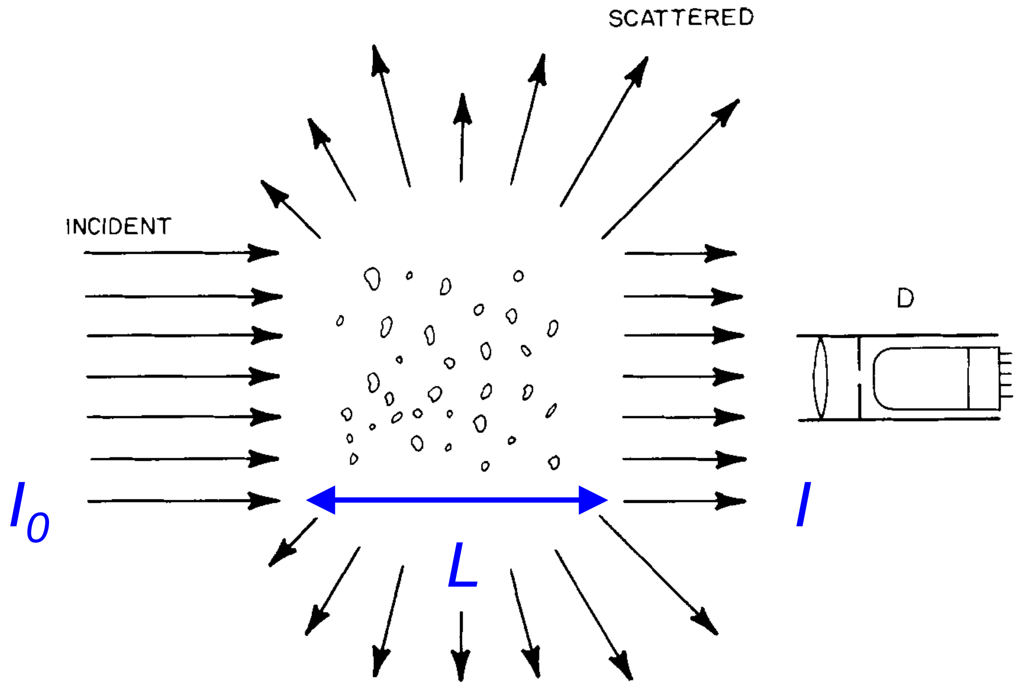

The attenuation of light along the direction of propagation through a scattering and absorbing medium is a key process responsible for visibility degradation.

The light attenuation for a parallel beam of light of incident irradiance I_0 is given by the Lambert-Beer law

$$\frac{I}{I_0} = e^{-\sigma_{ext} L}$$

σ_{ext} = extinction coefficient in m^{-1} ; L = length of atmospheric column in m

Mechanisms of interaction

When a beam of light impinges on a particle, electric charges in the particle are excited into oscillatory motion.

The excited electric charges reradiate energy in all directions (*scattering*) and may convert a part of the incident radiation into thermal energy (*absorption*).

Electromagnetic radiation transports energy. The amount of energy crossing an unit area perpendicular to the direction of propagation per time is its irradiance I_0 in W m^{-2}. The radiation W scattered or absorbed by a particle is proportional to I_0

$$W_{scat} = N\, C_{scat}\, I_0 \quad , \quad W_{abs} = N\, C_{abs}\, I_0$$

C_{scat} and C_{abs} in units of m^2 are the single-particle scattering and absorption cross sections.

Conservation of energy requires that the light removed from the incident beam by the particle is accounted for by scattering in all directions and absorption. The combined effect is referred to as *extinction*

$$C_{ext} = C_{scat} + C_{abs}$$

The *scattering efficiency* of a particle of cross-sectional area A_p is defined as

$$Q_{scat} = C_{scat} / A_p \Rightarrow Q_{ext} = Q_{scat} + Q_{abs}$$

The extinction coefficient σ_{ext} for an aerosol consisting of *N* particles per unit volume of cross-sectional area A_p (spherical particle of diameter D_p) is

$$\sigma_{ext} = N\,A_p\,Q_{ext} = N\,\frac{\pi\,D_p^{\;2}}{4}\,Q_{ext}$$

Particles may extinguish radiation by scattering and/or absorption according to

$$\sigma_{ext} = \sigma_{scat} + \sigma_{abs}$$

The fraction of scattering to extinction is defined by the single-scattering albedo

$$\omega_0 = \frac{\sigma_{scat}}{\sigma_{ext}} = \frac{\sigma_{scat}}{\sigma_{scat} + \sigma_{abs}} = 1 - \frac{\sigma_{abs}}{\sigma_{scat} + \sigma_{abs}}$$

Key Parameters

- ratio of particle size to wavelength of light, or *size parameter* $\alpha = \frac{\pi\,D_p}{\lambda}$
- complex index of refraction $m = n + i\,k$

  for non-absorbing particles is $k = 0$
  and for absorbing particles is $k > 0$
  m is determined by the chemical composition of the particle

TABLE 22.2 Refractive Indices of Atmospheric Substances at $\lambda = 589$ nm (Unless Otherwise Indicated)

	$m = n - ik$		
Substance	n	k	
Water	1.333	0 (see Table 22.1)	
Water (ice)	1.309		
NaCl	1.544	0	
H_2SO_4	1.426[a]	0	
NH_4HSO_4	1.473[b]	0	
$(NH_4)_2SO_4$	1.521[b]	0	
SiO_2	1.55	0	($\lambda = 550$ nm)
Carbon	1.96	0.66	($\lambda = 550$ nm)
Mineral dust[c]	1.56	−0.006	($\lambda = 550$ nm)

[a] Stelson (1990), assuming a 97% pure (by mass) mixture of H_2SO_4 with H_2O.
[b] Weast (1987).
[c] Tegen et al. (1996).

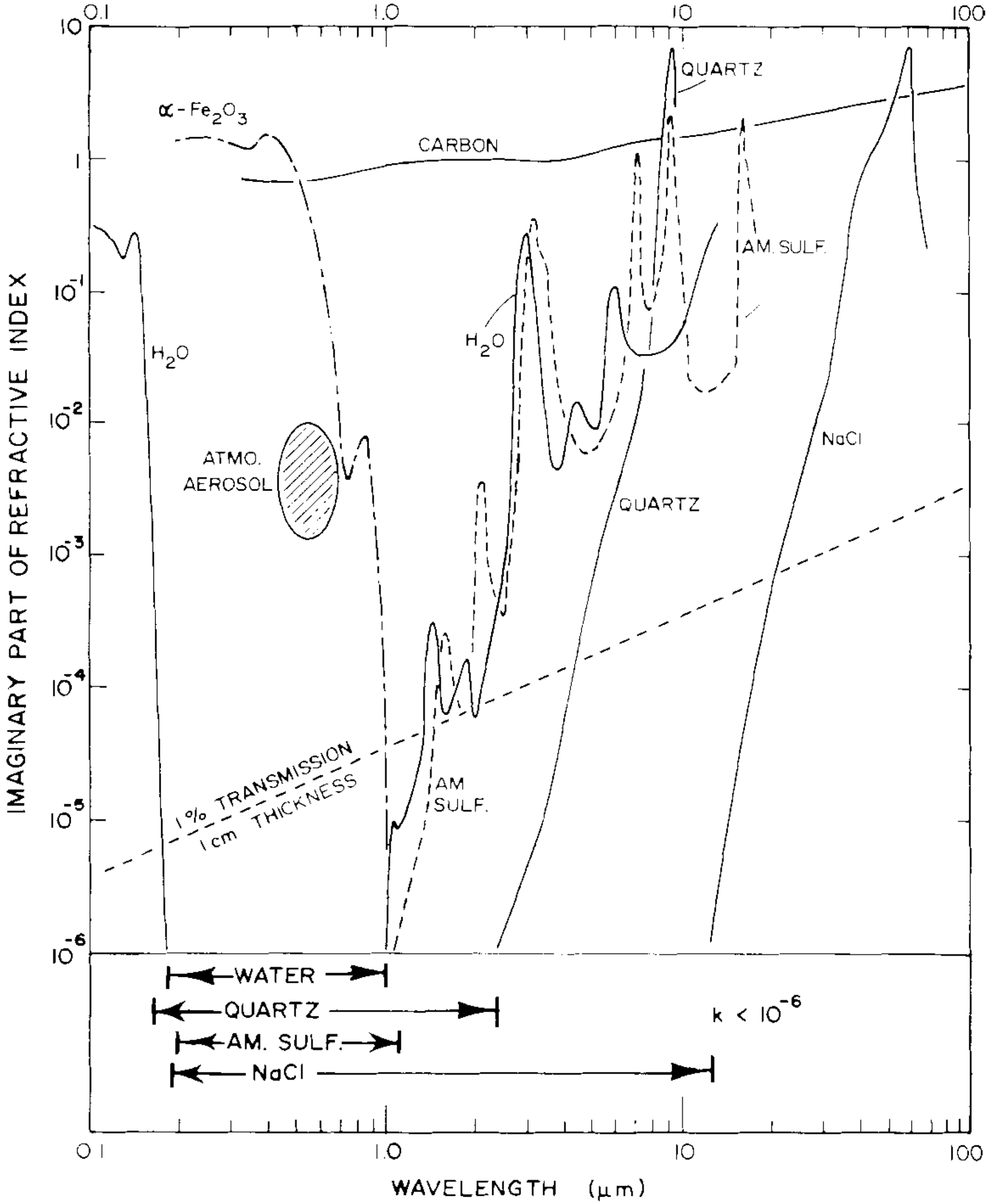

Light-absorbing aerosol components

visible + IR	Black Carbon
"green"	Fe_2O_3
near IR	H_2O
	$(NH_4)_2\ SO_4$
9 μm	SiO_2

In the visible spectral region, only graphitic-like black carbon absorbs light very efficiently;

in the graphite lattice, a two-dimensional free electron gas can interact almost perfectly with the electro-magnetic radiation.

Scattering and absorption by a sphere

Scattering and absorption cross sections can be calculated exactly for spherical particles by solving the electromagnetic wave equations for a spherical boundary, as presented by Gustav Mie in 1908.

Numerical Mie codes are widely used for the calculation of particle scattering and absorption properties, see Bohren and Huffman, 1983.

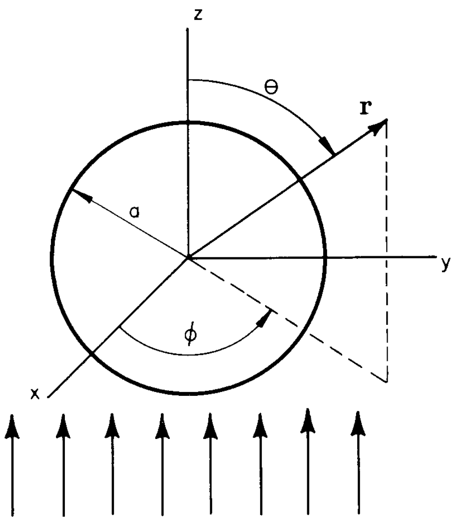

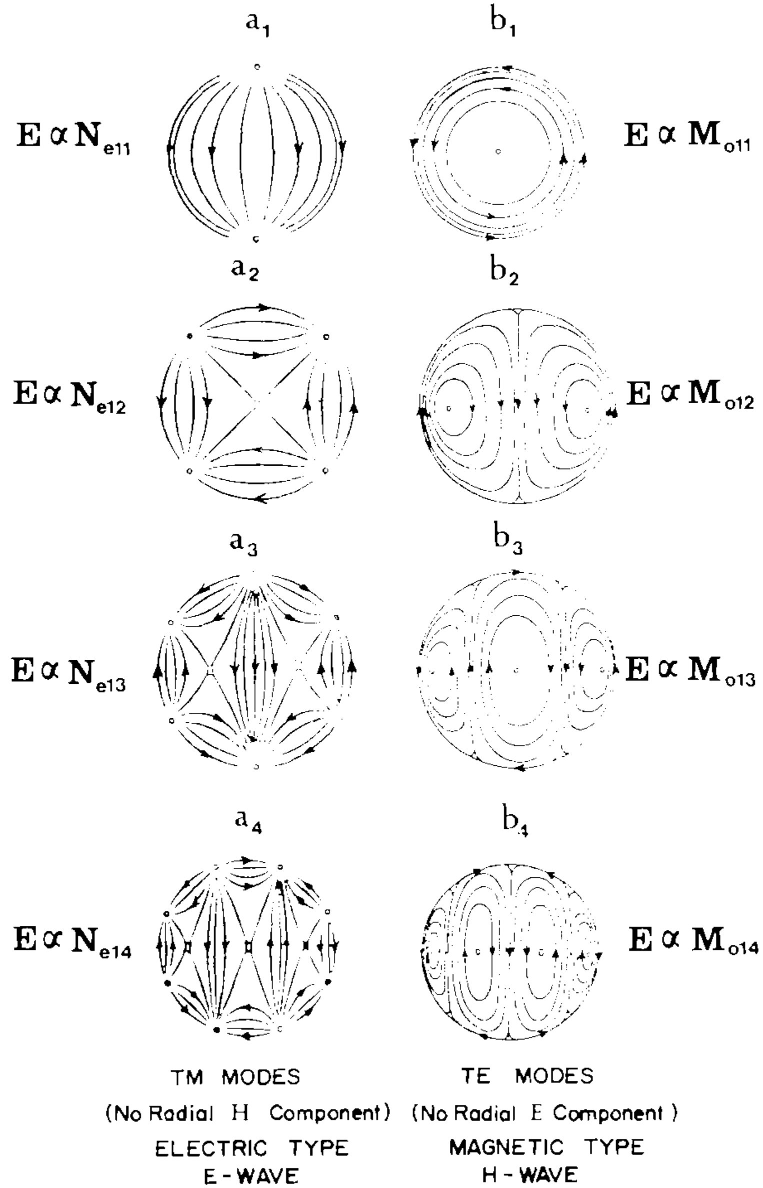

Summary of Mie Theory

(Bohren and Huffmann, 1983)

The angular distribution of scattered light of a polarised plane wave is

$$S_1 = \sum_n^\infty \frac{2n+1}{n(n+1)} \left(a_n \, \pi_n + b_n \, \tau_n\right)$$

$$S_2 = \sum_n^\infty \frac{2n+1}{n(n+1)} \left(a_n \, \tau_n + b_n \, \pi_n\right)$$

$$a_k = \frac{\alpha \, \psi_k'(\alpha \, m) \, \psi_k(\alpha) - \alpha \, m \, \psi_k'(\alpha) \, \psi_k(\alpha \, m)}{\alpha \, \psi_k'(\alpha \, m) \, \varsigma_k(\alpha) - \alpha \, m \, \varsigma_k'(\alpha) \, \psi_k(\alpha \, m)}$$

$$b_k = \frac{\alpha \, m \, \psi_k'(\alpha \, m) \, \psi_k(\alpha) - \alpha \, \psi_k'(\alpha) \, \psi_k(\alpha \, m)}{\alpha \, m \, \psi_k'(\alpha \, m) \, \varsigma_k(\alpha) - \alpha \, \varsigma_k'(\alpha) \, \psi_k(\alpha \, m)}$$

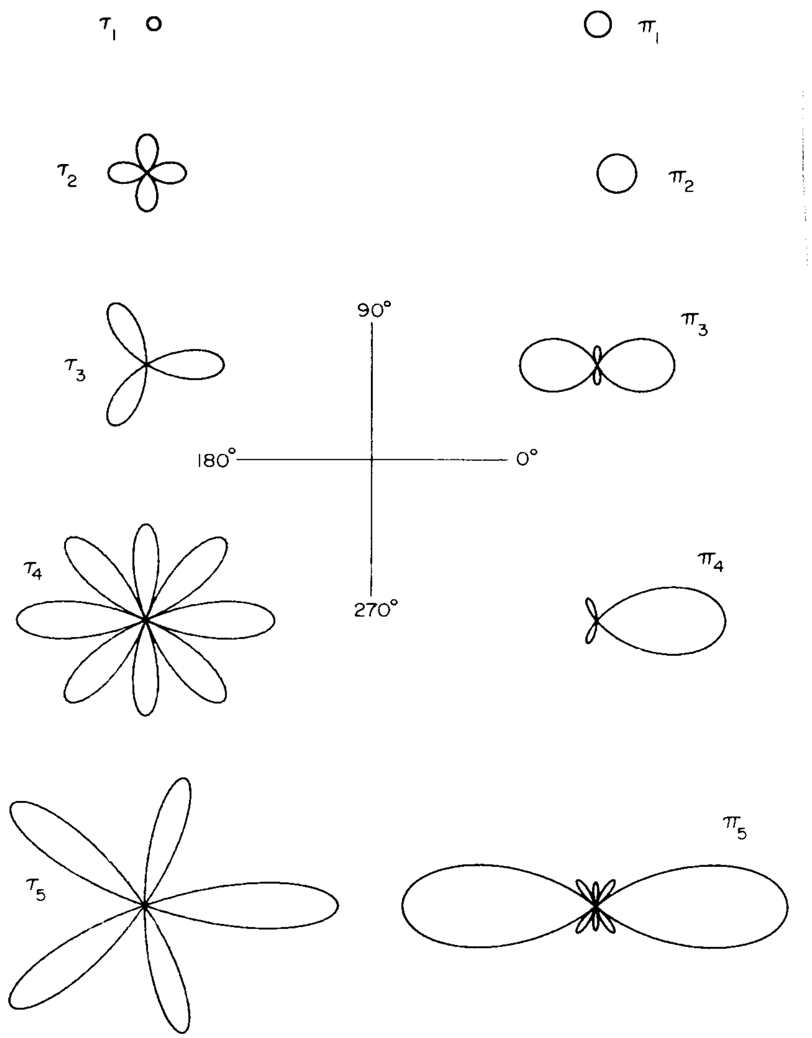

Integral Mie scattering and extinction cross sections are calculated from

$$C_{scat}\,(m,\alpha) = \int_0^{2\pi}\int_0^{\pi} \frac{\left|S(\theta,\phi)\right|^2}{k^2} \sin\theta\, d\theta\, d\phi$$

$$C_{ext}\,(m,\alpha) = \frac{4\pi}{k^2}\,\mathrm{Re}\,\left\{S(\theta = 0°)\right\}$$

$$C_{scat}\,(m,\alpha) = \frac{2\pi}{k^2} \sum_{n=1}^{\infty} (2n+1) \left[\left|a_n\right|^2 + \left|b_n\right|^2\right]$$

$$C_{ext}\,(m,\alpha) = \frac{2\pi}{k^2} \sum_{n=1}^{\infty} (2n+1)\,\mathrm{Re}\,\left\{a_n + b_n\right\}$$

with wave number *k* and size parameter

$$\alpha = \frac{\pi\, D_p}{\lambda}$$

α << 1 Rayleigh scattering regime

α ≅ 1 Mie scattering regime

α >> 1 Geometrical optics regime

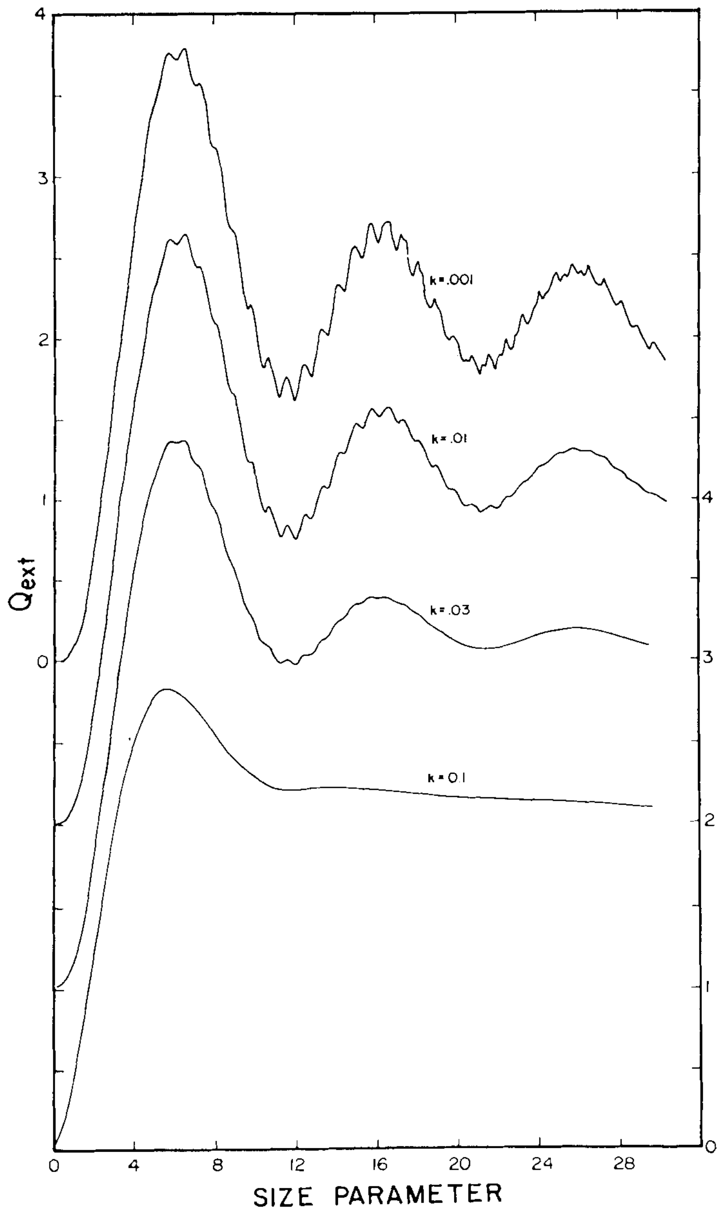

Rayleigh scattering regime

With respect to visible radiation, particles of diameter ≤ 0.1 µm lie in the Rayleigh regime.

The angular distribution of scattered radiation is symmetrical in the forward and backward direction with respect to the incident light beam and almost independent of particle shape.

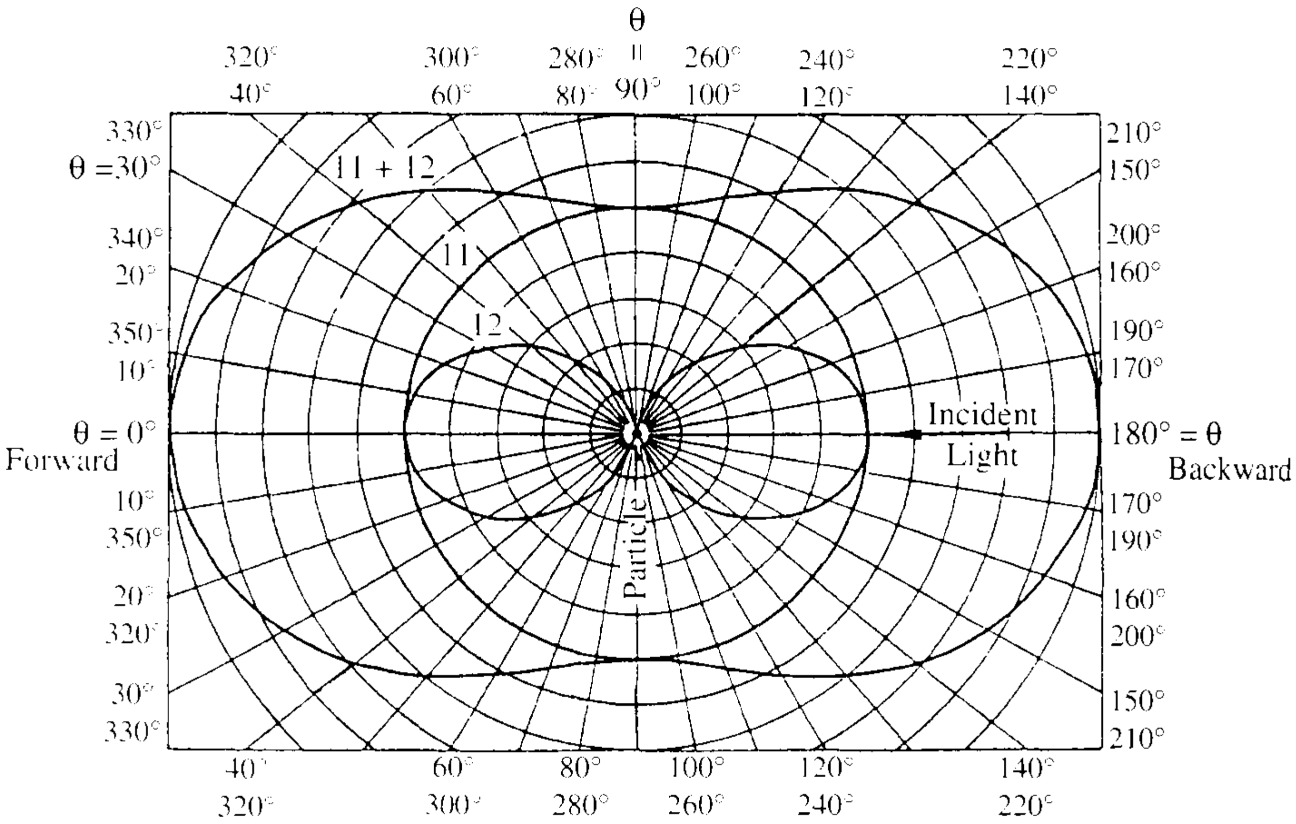

Extinction, scattering and absorption efficiencies or small particles

Efficiencies are calculated from the power series expansions of the spherical Bessel functions from Mie theory, when only the first two terms of the power series expansion are considered:

$$Q_{scat}\,(m,\alpha) = \frac{8}{3}\,\alpha^4\,\left|\frac{m^2-1}{m^2+2}\right|^2$$

$$Q_{abs}\,(m,\alpha) \cong 4\,\alpha\,\mathrm{Im}\left\{\frac{m^2-1}{m^2+2}\right\}$$

$$Q_{ext}\,(m,\alpha) = Q_{scat}\,(m,\alpha) + Q_{abs}\,(m,\alpha)$$

Thus, for sufficiently small particles

$$Q_{scat}\,(m,\alpha) \propto \left(\frac{D_p}{\lambda}\right)^4 \;;\; C_{scat} = \frac{\pi\,D_p^2}{4} Q_{scat} \;\Rightarrow\; \frac{C_{scat}}{V_p} \propto \frac{D_p^3}{\lambda^4}$$

$$Q_{abs}\,(m,\alpha) \propto \frac{D_p}{\lambda} \;;\; C_{abs} = \frac{\pi\,D_p^2}{4} Q_{abs} \;\Rightarrow\; \frac{C_{abs}}{V_p} \propto \frac{1}{\lambda}$$

Mass-specific coefficients

Extinction, scattering and absorption efficiencies normalised to particle mass, calculated for green light at λ = 550 nm:

Rayleigh-regime $D_p << \lambda$

C_{abs} / Volume independent of D_p
C_{scat} / Volume $\propto D_p^3$

Geometrical Optics $D_p >> \lambda$

$C_{scat,\,abs}$ / Volume $\propto D_p^{-1}$

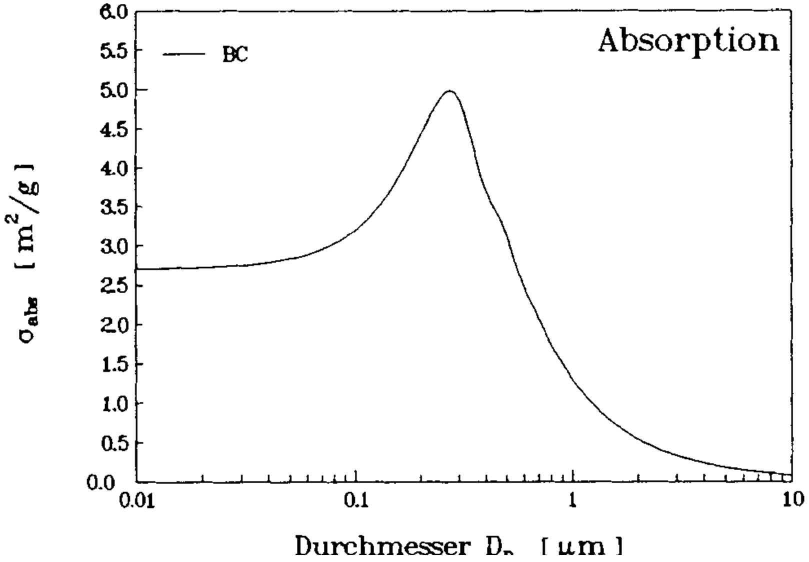

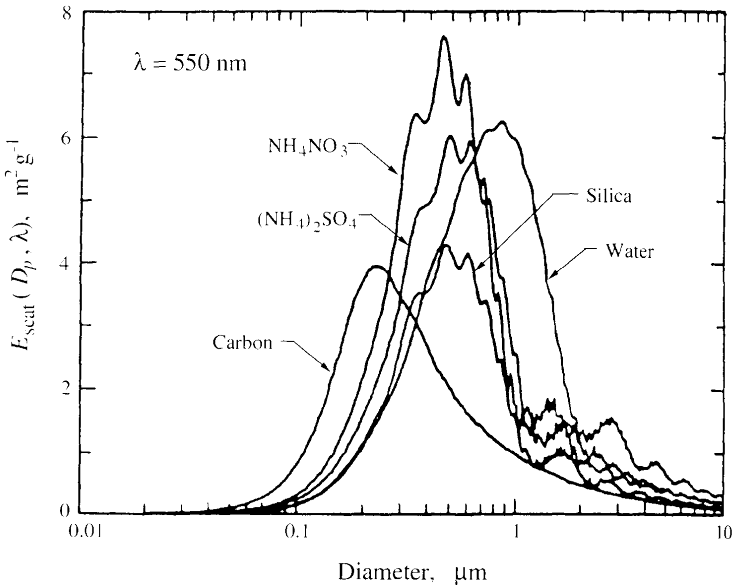

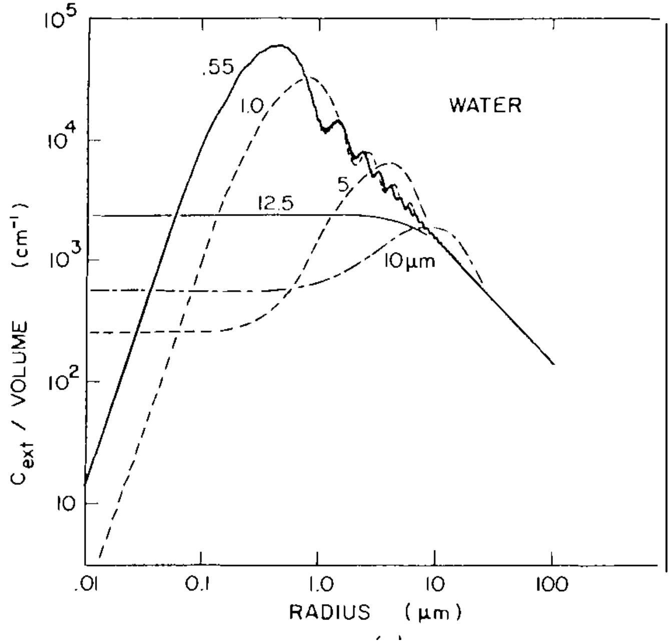

Measurement of the Extinction Coefficient

The aerosol extinction coefficient is measured in a cavity of sufficient length by determining the light attenuation along the optical path. The light attenuation for a parallel beam of light of incident irradiance I_0 is given by the Lambert-Beer law

$$\frac{I}{I_0} = e^{-\sigma_{ext} L}\,; C_{ext}\,(m,\alpha) = \frac{4\pi}{k^2}\,\mathrm{Re}\,\{S(\theta = 0°)\};\quad \sigma_{ext} = \int C_{ext}\,(m,\alpha)\,n_N\,(D_p)\,d\,\log D_p$$

σ_{ext} = extinction coefficient in m^{-1} ; L = length of atmospheric column in m

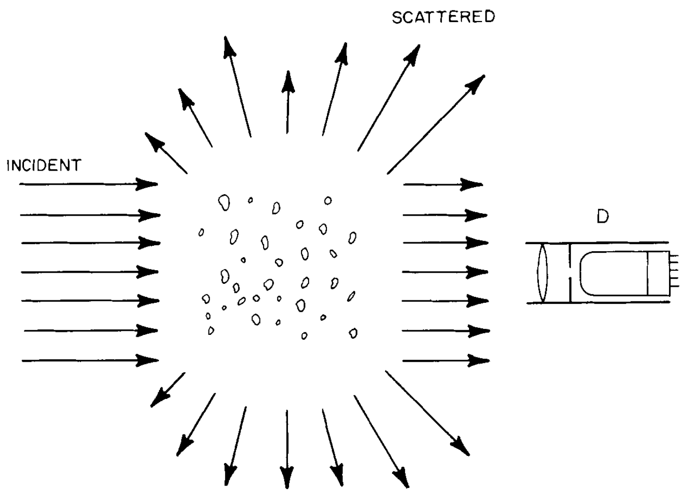

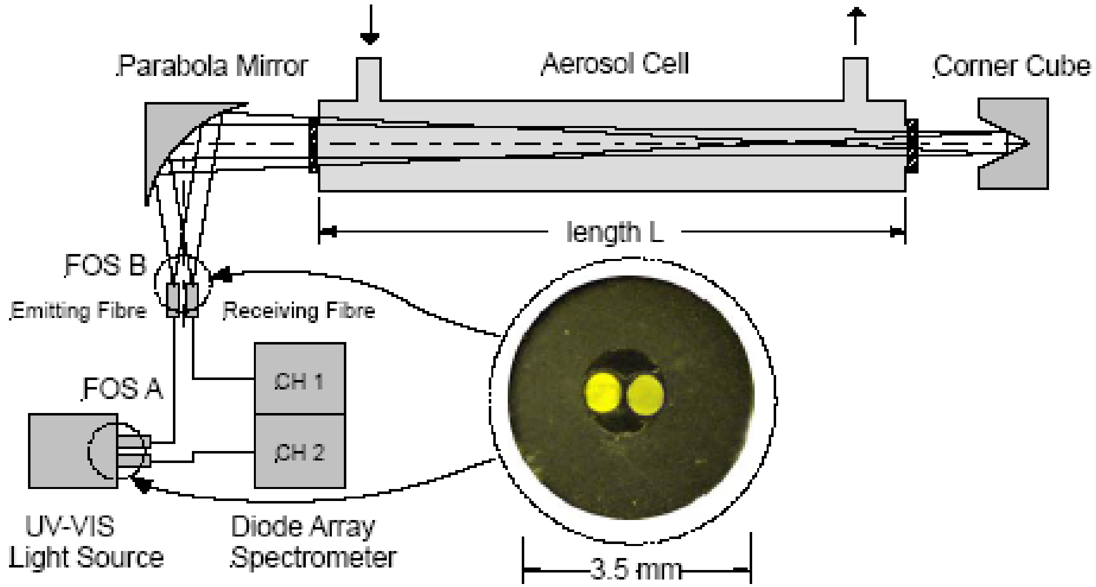

Long path extinction spectrometer of Research Centre Karlsruhe, Martin Schnaiter.

Measurement of the Scattering Coefficient

The aerosol scattering coefficient is measured in an integrating nephelometer which determines the amount of light scattered in all angles. The light scattering coefficient is given by

$$C_{scat}(m,\alpha) = \int_0^{2\pi}\int_0^{\pi} \frac{|S(\theta,\phi)|^2}{k^2} \sin\theta \, d\theta \, d\phi \quad ; \quad \sigma_{scat} = \int C_{scat}(m,\alpha)\, n_N(D_p)\, d\log D_p$$

Integration of scattered light is achieved by collecting light scattered in all solid angles. Data analysis requires correction of truncation angles in the forward direction.

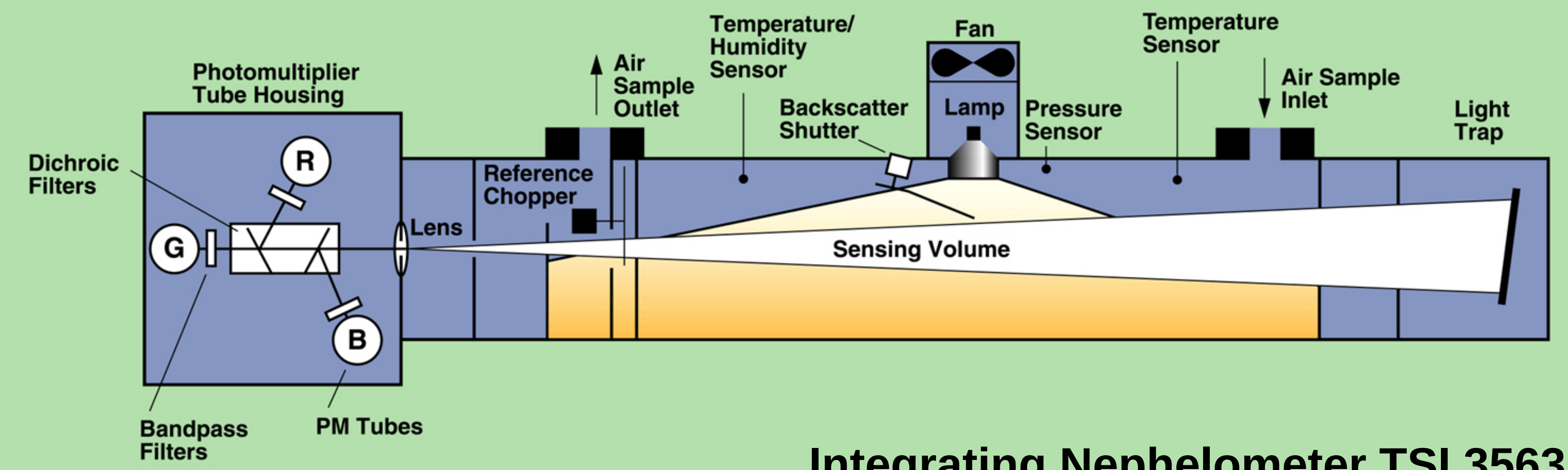

Integrating Nephelometer TSI 3563

Aerosol Absorption Measurement Methods

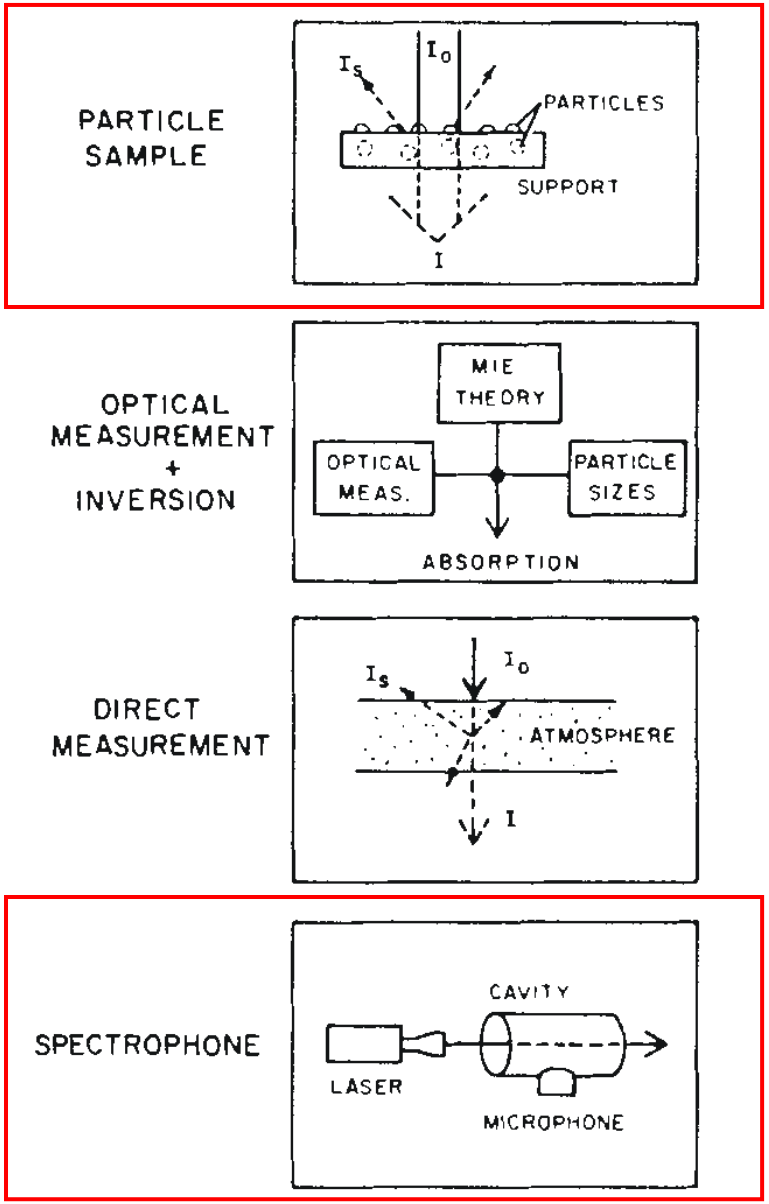

Sketches of the major categories of measuring light absorption by aerosol particles, the graph is taken from the Proceedings of the First International Workshop on Light Absorption by Aerosol Particles

(Gerber, H.E. and E.E. Hindman (1982) *Light Absorption by Aerosol Particles*, Spectrum Press, Hampton.).

Filter-based Aerosol Absorption Measurement Methods

- Sampling of particles on a fibrous filter matrix.
- Measurement of the modification of filter-optical properties by the collected aerosol particles.
- Assumption of Lambert-Beer type relationship for data analysis.

Transmission method

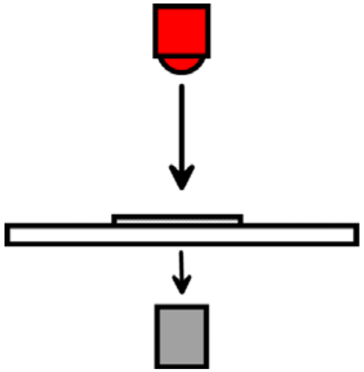

Reflectance method

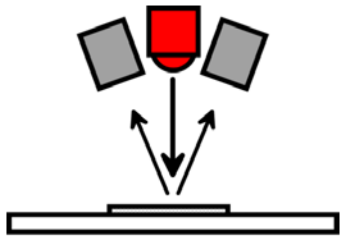

$$ATN = -100\ \ln\left(\frac{T}{T_0}\right) = B_{ATN}\ S_{BC}$$

$$\sigma_{0\ (TRANS)} = \frac{A}{V}\ \ln\left(\frac{T_0}{T}\right)$$

$$\sigma_{0\ (REF)} = \frac{1}{2}\frac{A}{V}\ln\left(\frac{R_0}{R}\right)$$

filter surface area A , sampled volume V, mass-specific absorption coefficient B_{ATN} [$m^2\ g^{-1}$] , filter mass loading S_{BC} [$\mu g/cm^2$]

Interaction of Particles, Fibres and Radiation

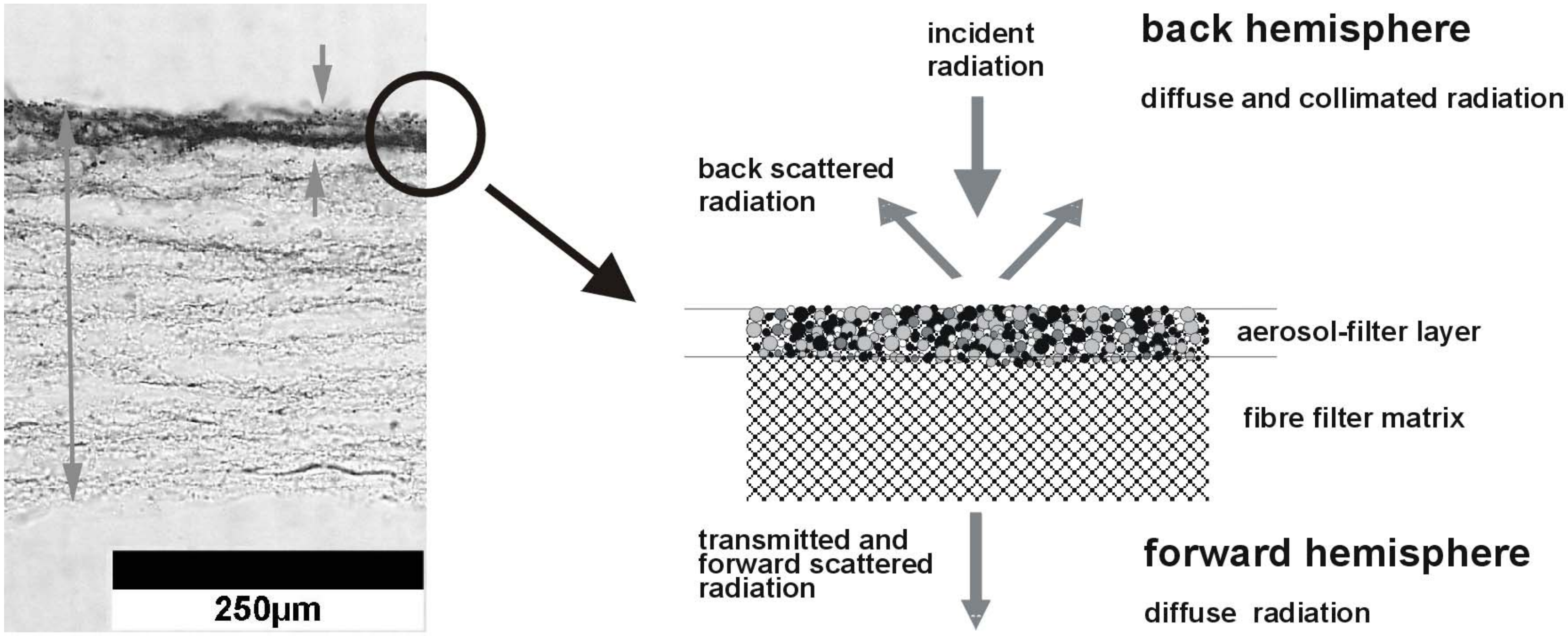

Filter Matrix Effects

+ Multiple scattering of light by filter fibres and light-scattering aerosol particles tends to overestimate the absorption coefficient.

- „Shadowing“ of collected particles inside the fibre matrix tends to underestimate the absorption coefficient .

Multi-Angle Absorption Photometry

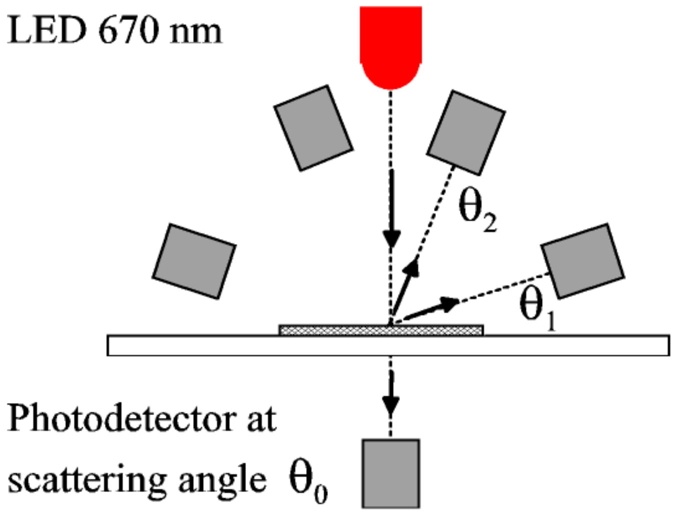

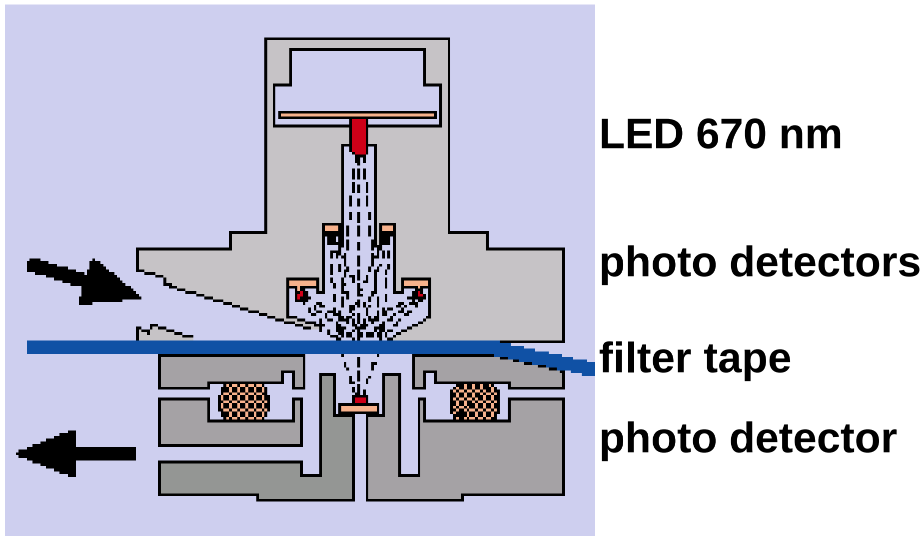

The MAAP sensor unit permits the simultaneous analysis of transmittance method, reflectance method and multi-angle absorption photometry from the same aerosol sample.

Petzold, A. and M. Schönlinner,
J. Aerosol Sci., 35, 421-441, 2004.

RAOS 2002
Kerosene soot experiments

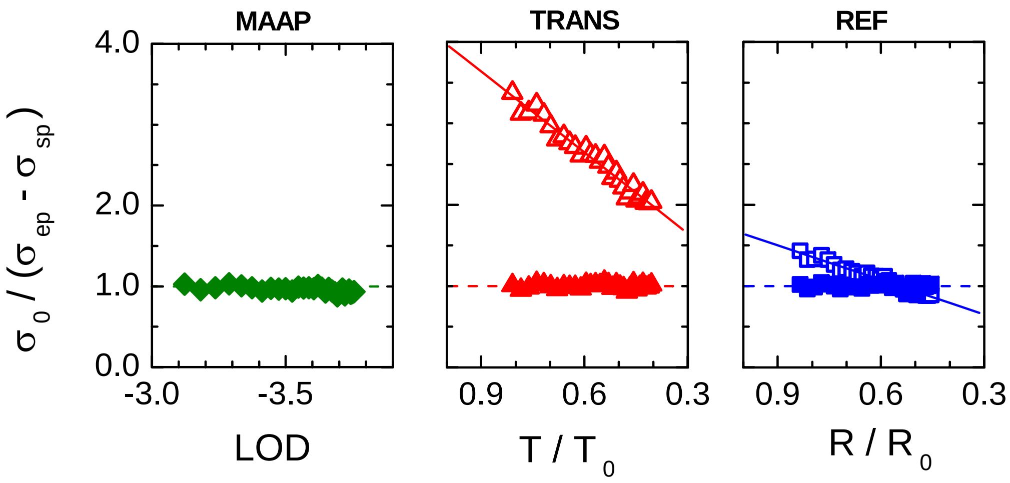

Correction functions for filter loading effects, determined from pure combustion particles; reference absorption coefficient is $\sigma_{ap} = \sigma_{ep} - \sigma_{sp}$.

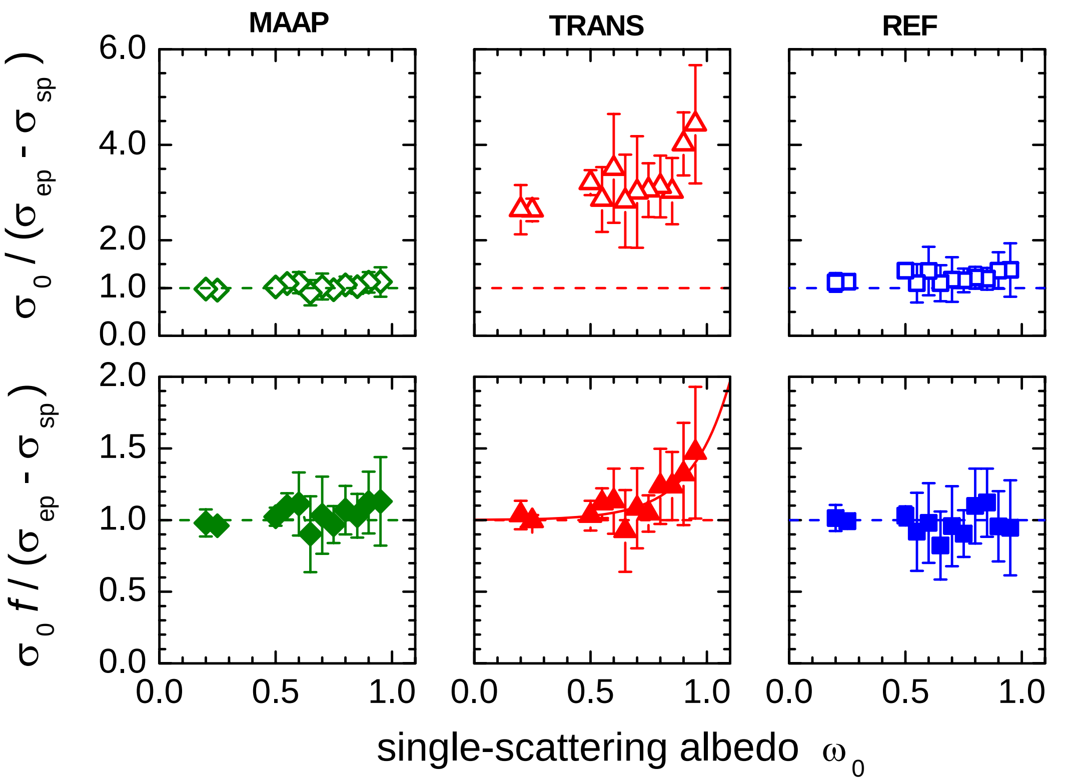

Correction functions for the effect of aerosol light scattering, determined from kerosene soot - ammonium sulphate mixtures

Petzold, A., H. Schloesser, P.J. Sheridan, W.P. Arnott, J.A. Ogren, and A. Virkkula, *Aerosol Sci. Technol.*, 39, 40-51, 2005.

RAOS 2002 Kerosene soot experiments

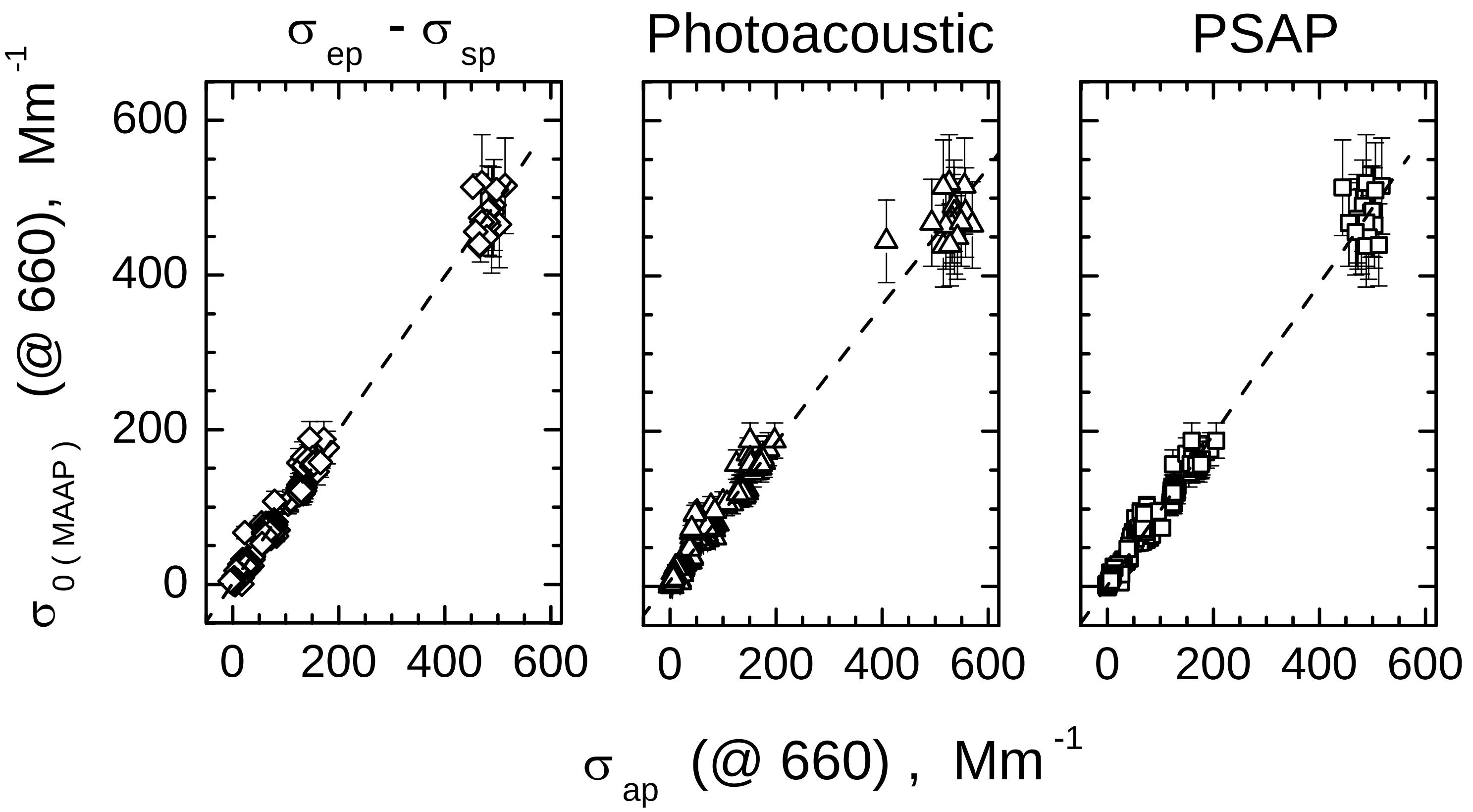

$$\sigma_{ext} = \sigma_{scat} + \sigma_{abs}$$

Particle Sizing by Light Scattering

Rayleigh Regime: Extinction, scattering and absorption efficiencies

Efficiencies are calculated from the power series expansions of the spherical Bessel functions in the coefficients a_n and b_n from Mie theory, when only the first two terms are considered:

$$Q_{scat}\,(m,\alpha) = \frac{8}{3}\,\alpha^4 \left|\frac{m^2-1}{m^2+2}\right|^2 \qquad Q_{scat}\,(m,\alpha) \propto \left(\frac{D_p}{\lambda}\right)^4 \;;\quad C_{scat} \propto \frac{D_p^6}{\lambda^4}$$

$$Q_{abs}\,(m,\alpha) \cong 4\,\alpha\,\mathrm{Im}\left\{\frac{m^2-1}{m^2+2}\right\} \qquad Q_{abs}\,(m,\alpha) \propto \frac{D_p}{\lambda} \;;\quad C_{abs} \propto \frac{D_p^3}{\lambda}$$

Angular distribution of radiation scattered by Rayleigh particles

The angular distribution of scattered radiation is symmetrical in the forward and backward direction almost independent of particle shape.

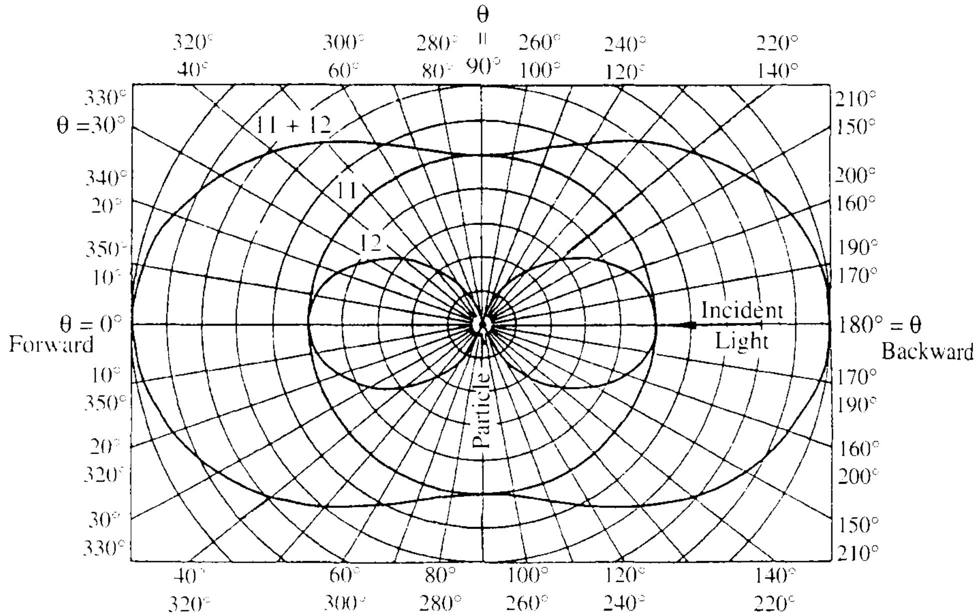

Angular distribution of radiation scattered by Mie particles

Polar plots of angular scattering by spheres with m = 1.33 (H_2O).

As size parameter x (α) increases by a factor of 20, forward-to-backward scattering increases by about 1000.

Particle sizing by Mie scattering requires careful modelling of instrument response functions R according to the scattering and detection geometry.

At distinct scattering angles, Mie ambiguities may results in unambiguous size-scattering relationships.

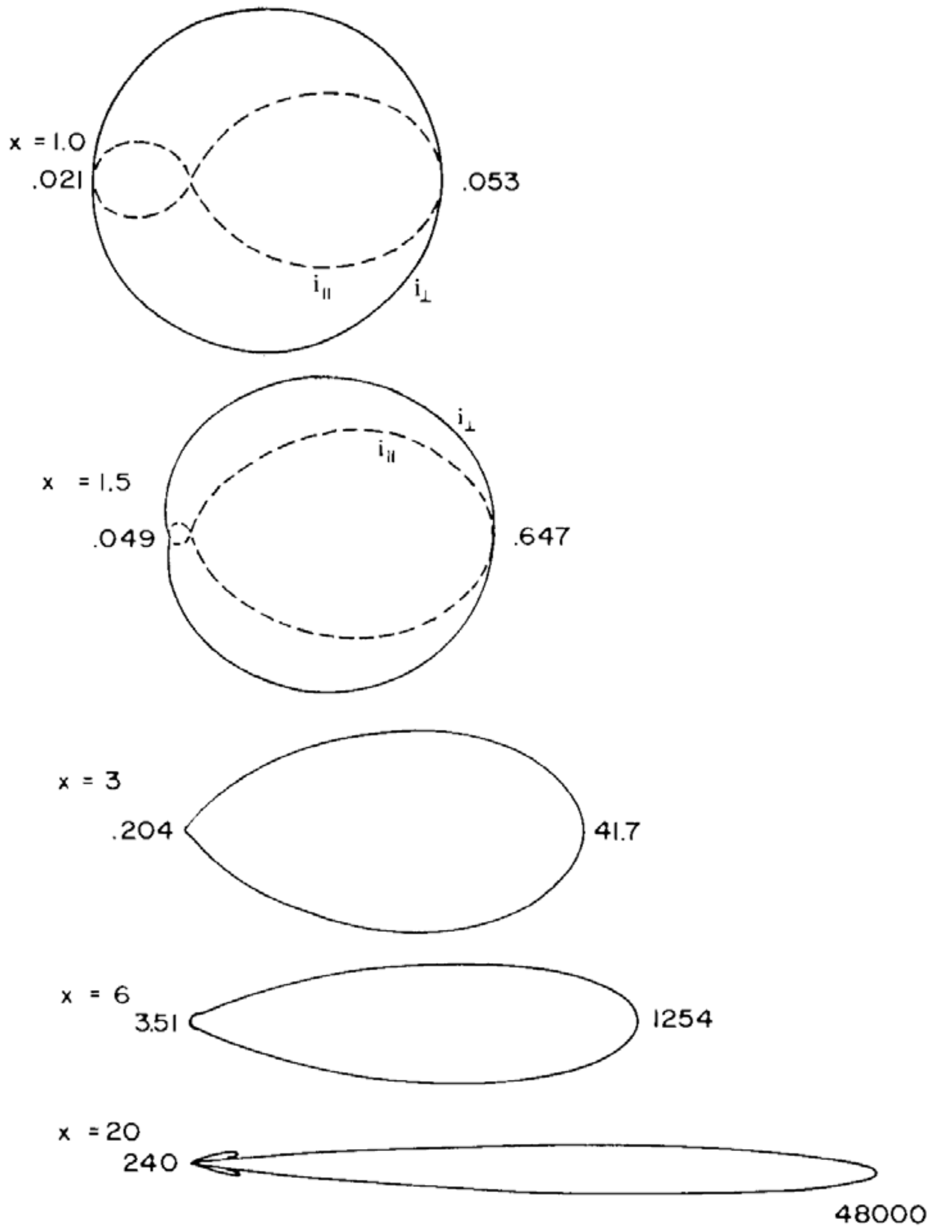

Optical Particle Counters

Principle of operation

- A dilute aerosol flow is directed through a laser beam
- Aerosol particles crossing the laser beam scatter light
- The scattered light is collected in a defined solid angle

Example: The Classical Scattering Aerosol Spectrometer Probe CSASP

radiatiopn source He-Ne laser 632 nm: scattering angle 4 - 22°

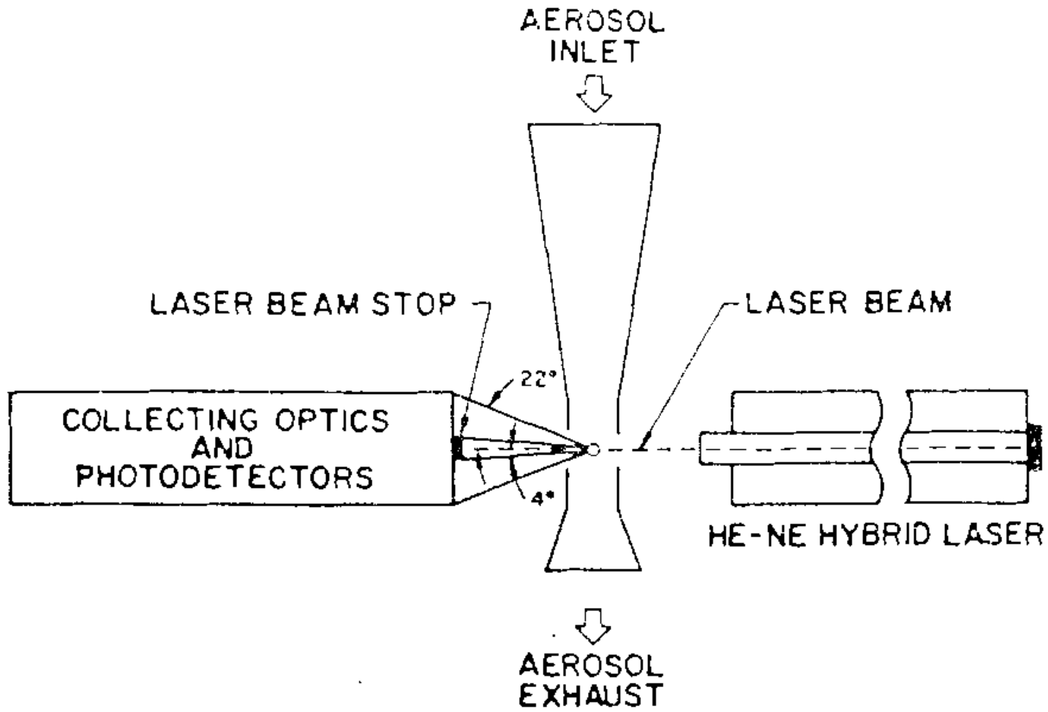

Table 2. Characteristics of Knollenberg light scattering aerosol counters

Instrument	Light source	Light-collecting optics* $\alpha-\beta$	Flow rate or active area
CSASP	5 mW He–Ne laser	4–22°	0.15 cm³/sec
ASASP	2 mW He–Ne laser (intra-cavity)	4–22°	0.1 cm³/sec
FSSP	5 mW He–Ne laser	3–13°	0.25 mm²†
ASSP‡	5 mW He–Ne laser	5.3–12.4°	0.4 mm²†

* All instruments have axial symmetry with respect to the direction of the laser source and the polar angles α, β refer to a cone subtending angles α through β from the direction of forward scattering.

† Flow rate can be determined from active area by multiplying by the speed at which air (containing aerosol) passes through the instrument.

‡ The manufacturer has produced two models of the ASSP having different optics, but only one of these has been studied here. The other collects light scattered 6.7°–14.4° from the direction of forward scattering.

Pinnick and Auvermann, J. Aerosol Sci., 10, 55-74, 1979.

Optical Particle Counters - Calibration Set-Up

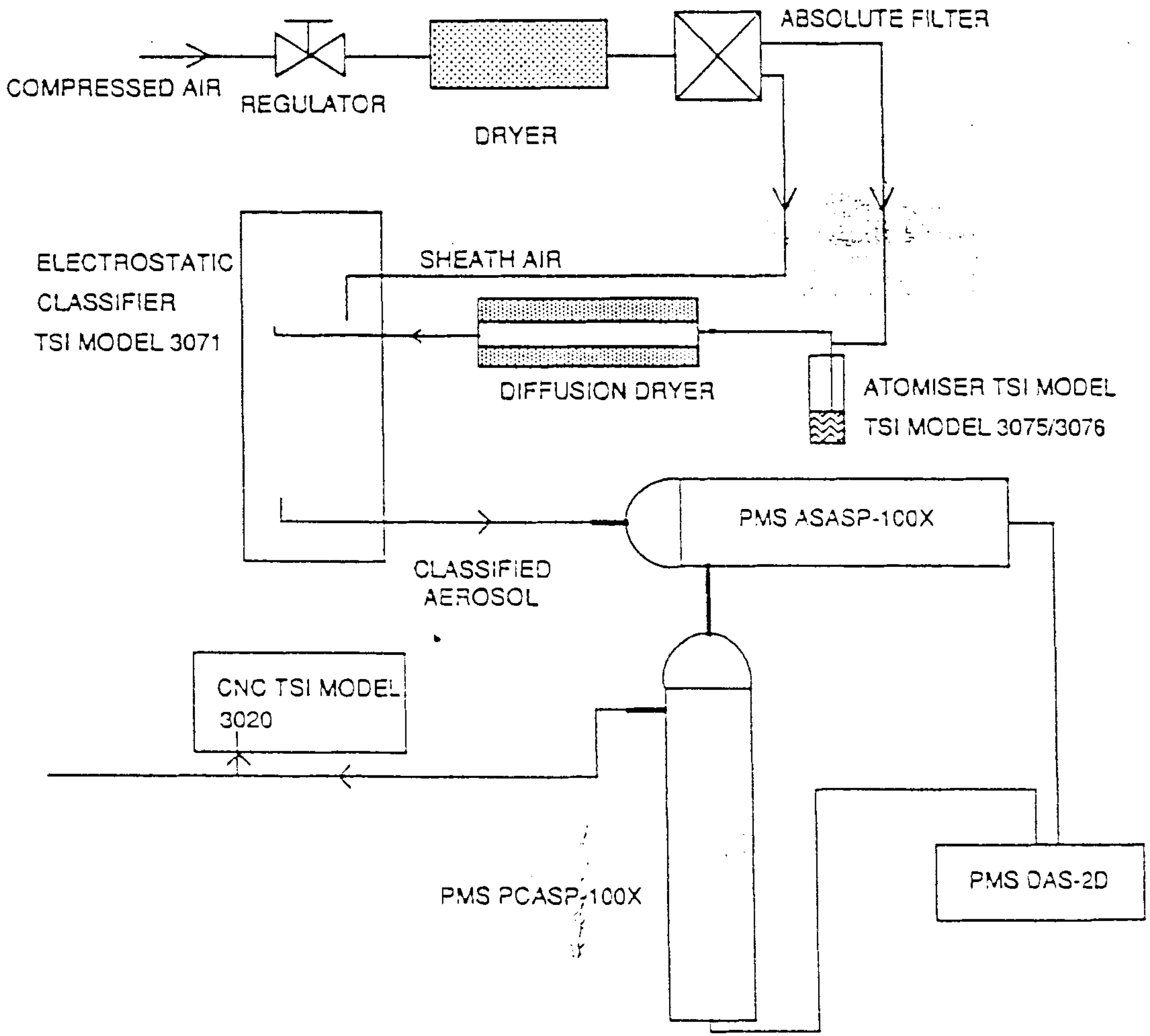

The Measurement Process

1/ Consider a set of 1000 particles.
2/ Determine the size of every particle by appropriate methods.
3/ Divide the entire size range into a series of successive particle size intervals
4/ Sort the particles according to their size.
5/ Plot the grouped data as a histogram of numbers of occurrence.

⇒ **Simplest form of a number size distribution**

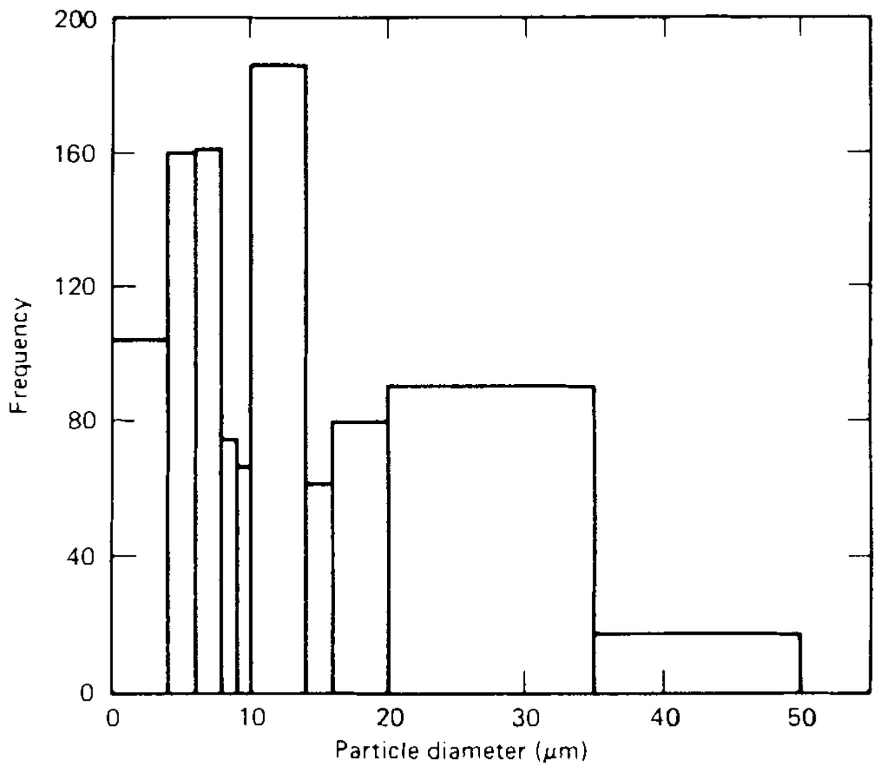

Height of the interval = number of particles in the size bin

Width of the interval = upper bound diameter - lower bond diameter

Intervals are not comparable because height depends on width.

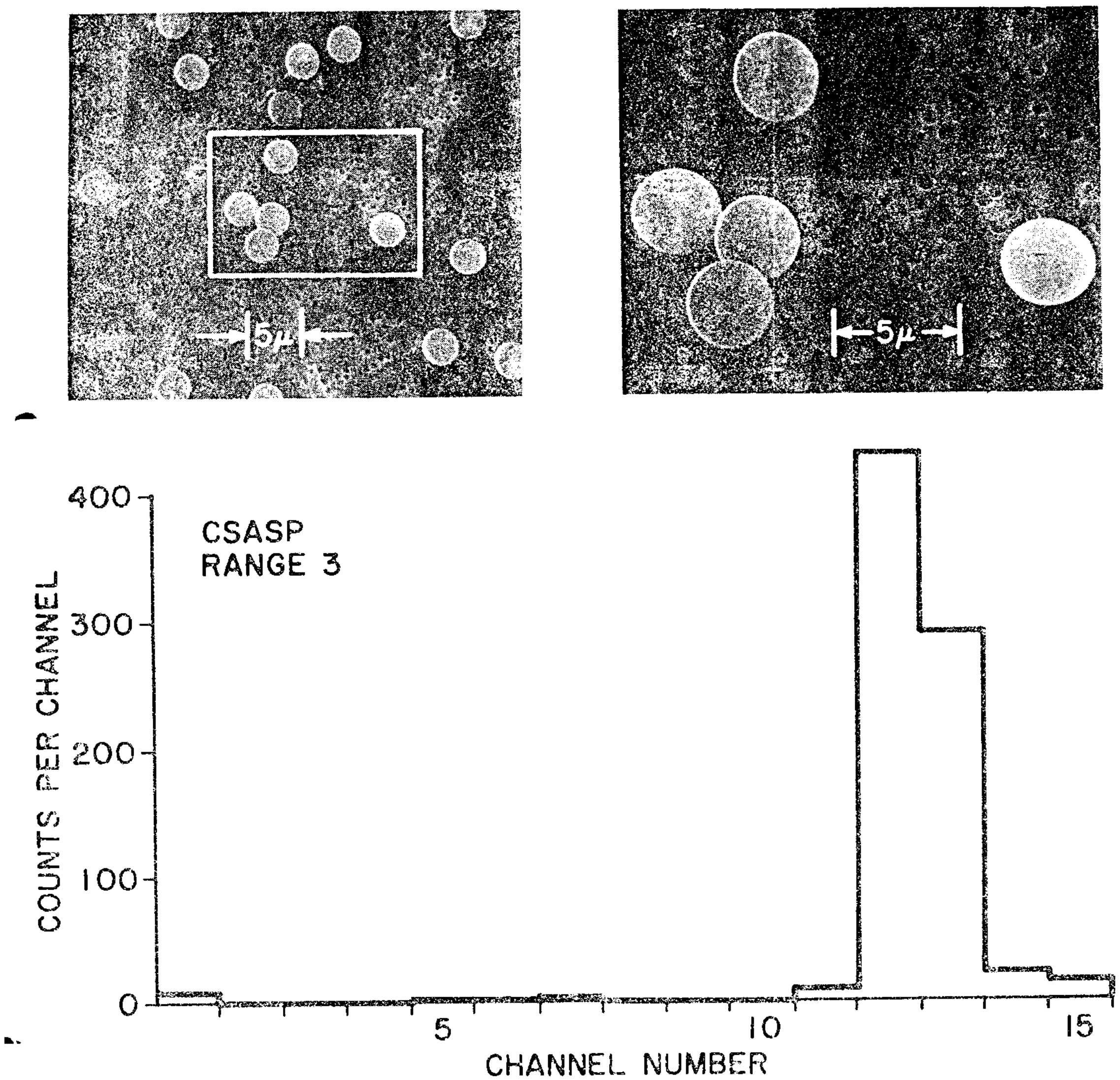

Calibration with solid spherical particles of nigrosin dye

Pinnick and Auvermann, J. Aerosol Sci., 10, 55-74, 1979.

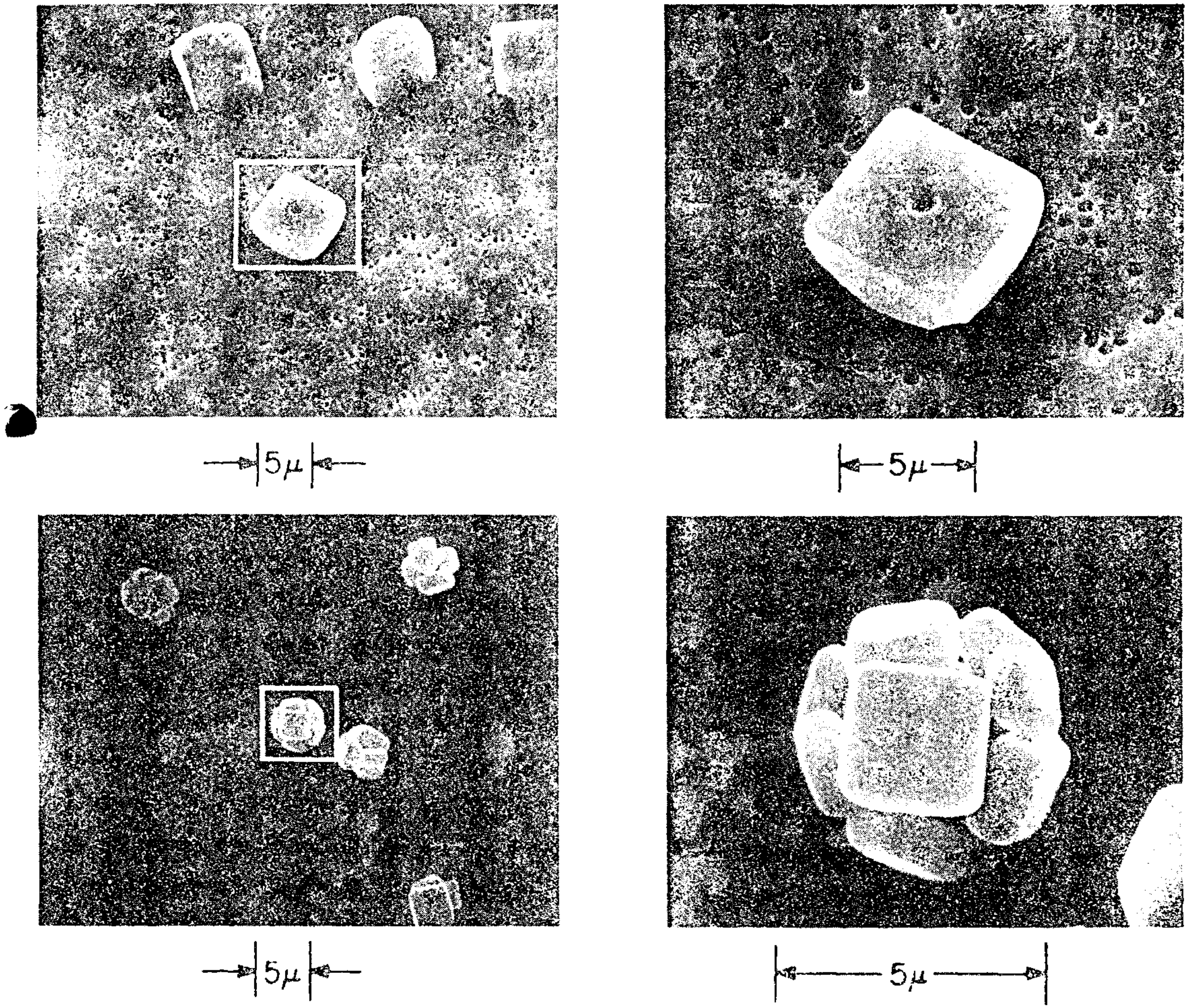

Irregularly shaped NaCl particles

Pinnick and Auvermann, J. Aerosol Sci., 10, 55-74, 1979.

FSSP - 300

Forward Scattering Spectrometer
Probe Type 300

scattering angle 5 - 12°

size range D = 0.3 - 20 µm

in situ measurement

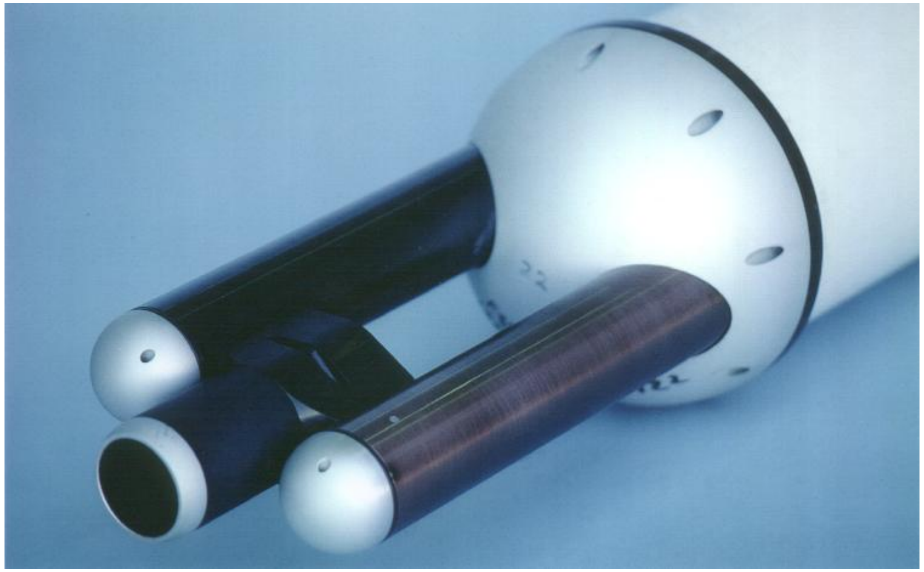

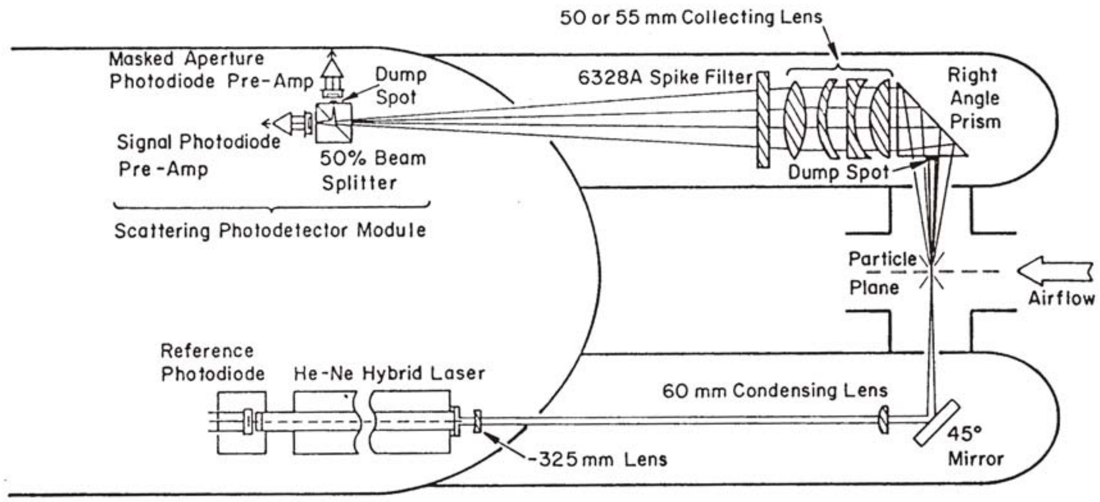

Probe Characteristics - FSSP

Consider scattering of particles in a plane wave of polarised radiation.
Ambiguities of Mie scattering concerning particle size have to be considered.

$$R_{FSSP} = \frac{\pi}{k^2} \int_{\theta_{\min}}^{\theta_{\max}} \left[\left| S_1(\theta) \right|^2 + \left| S_2(\theta) \right|^2 \right] \sin\theta \, d\theta$$

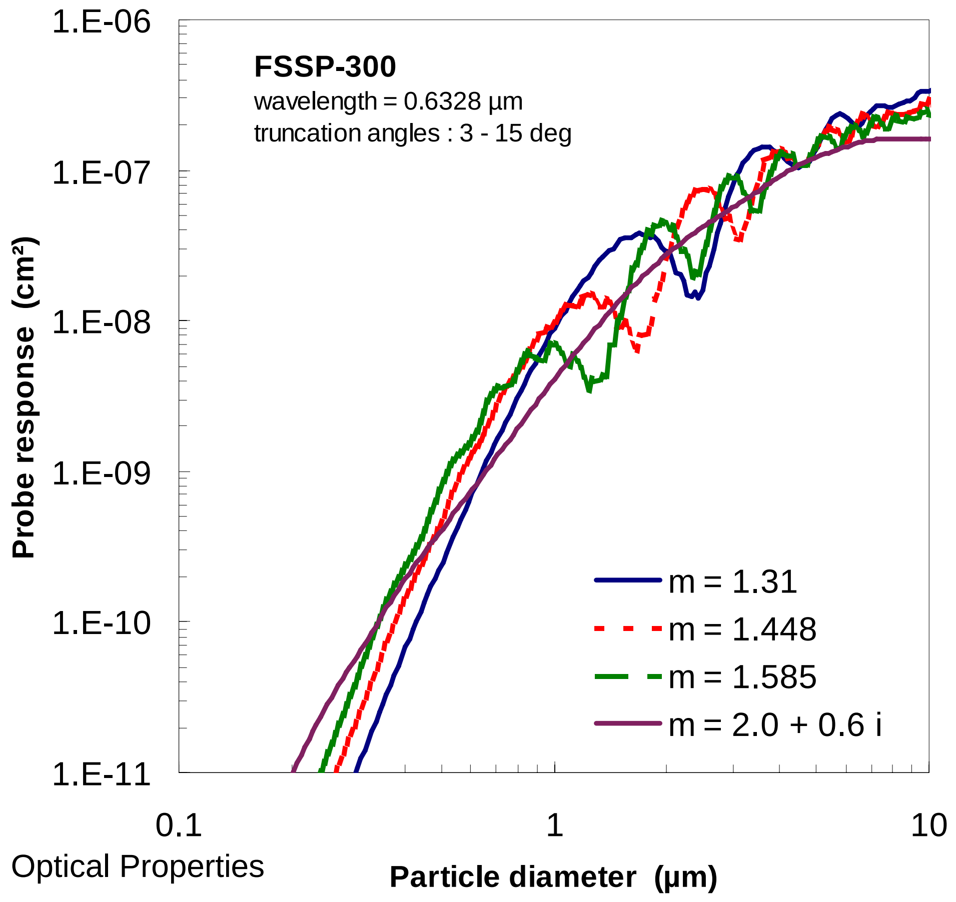

PCASP 100X

Passive Cavity Aerosol Spectrometer Probe

scattering angle 35 - 120°

size range D = 0.1 - 3 µm

measures dry aerosol

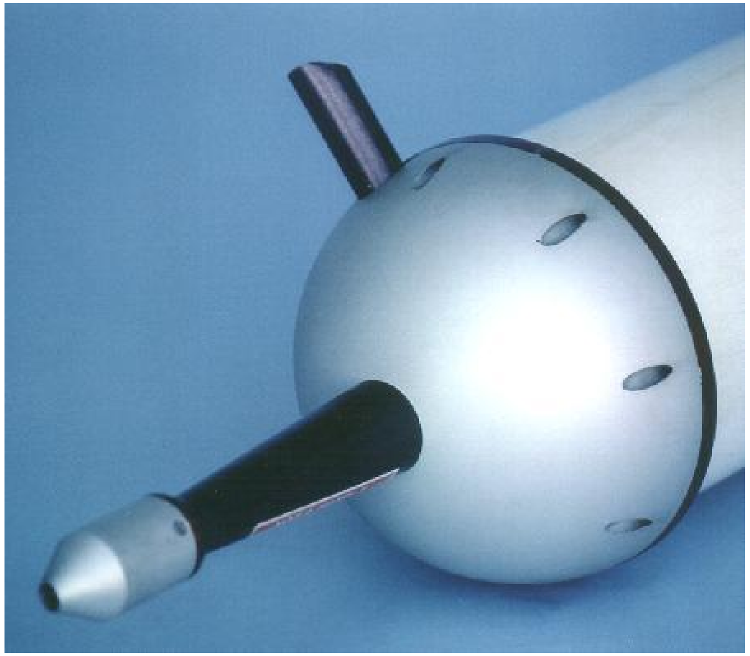

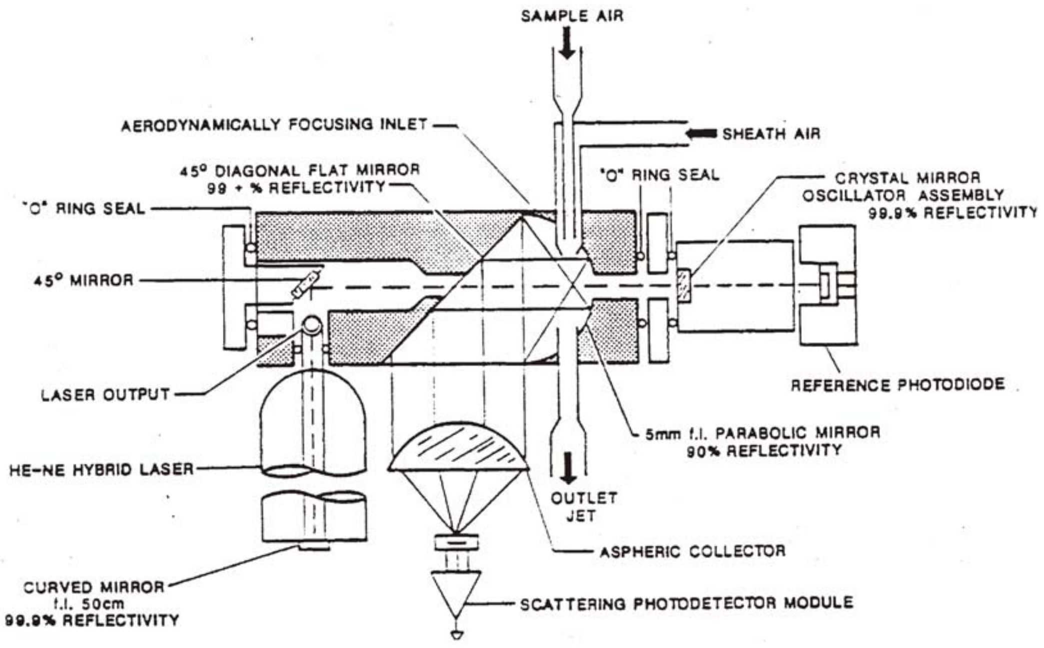

active sampling of aerosol

focusing of the aerosol by a dry sheath air flow

intensive radiation field generated by multiple reflections of the laser beam in a passive cavity outside the laser resonator.

Probe Characteristics - PCASP

Consider scattering of particles in a wave inside a reflector. Since mutiple reflection in the passive cavity do not generate coherent radiation, no standing wave is generated.

$$R_{PCASP} = \frac{\pi}{k^2} \int_{\theta_{\min}}^{\theta_{\max}} \left[\left|S_1(\theta)\right|^2 + \left|S_1(\pi-\theta)\right|^2 + \left|S_2(\theta)\right|^2 + \left|S_2(\pi-\theta)\right|^2 \right] \sin\theta \, d\theta$$

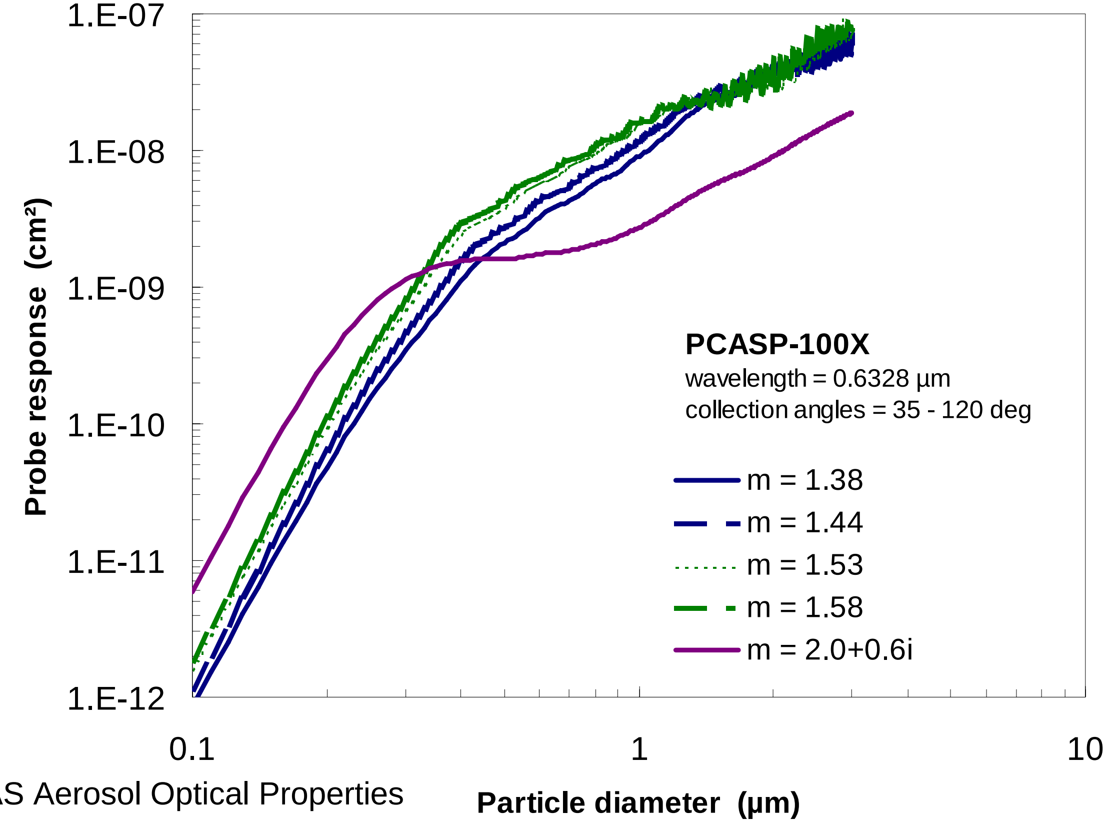

Calibration Studies

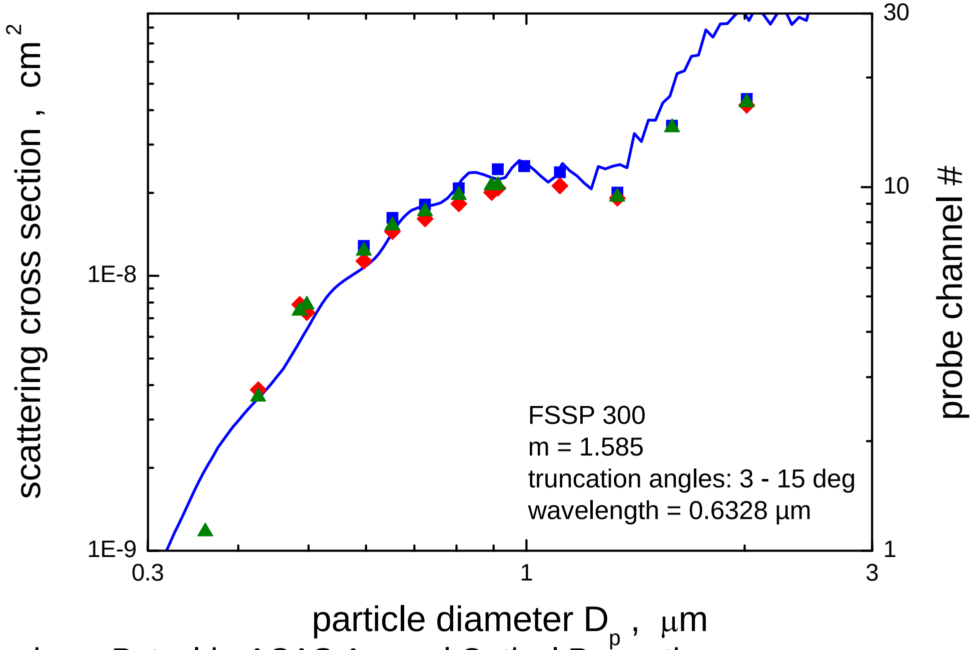

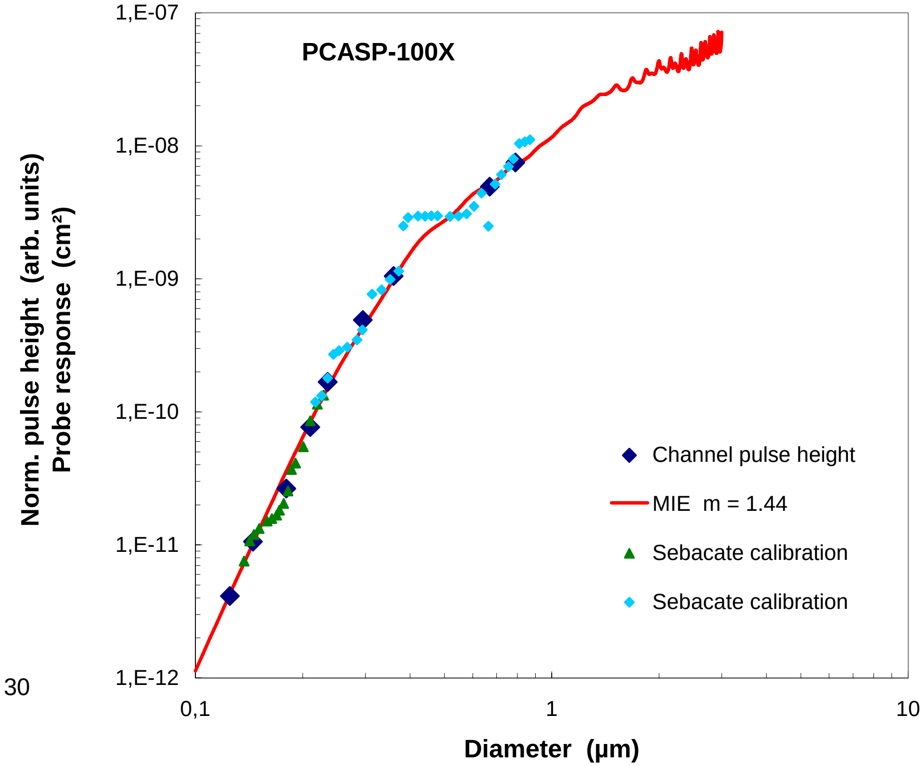

Application #1: Refractive Index Determination

INPUT DATA

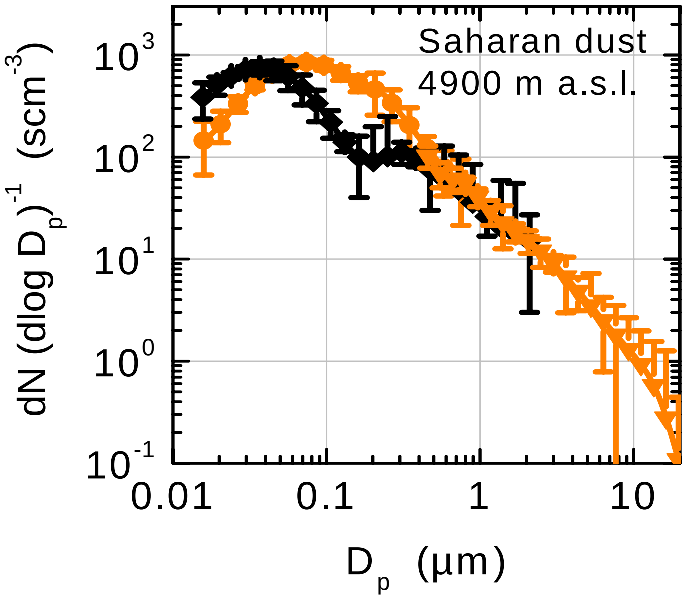

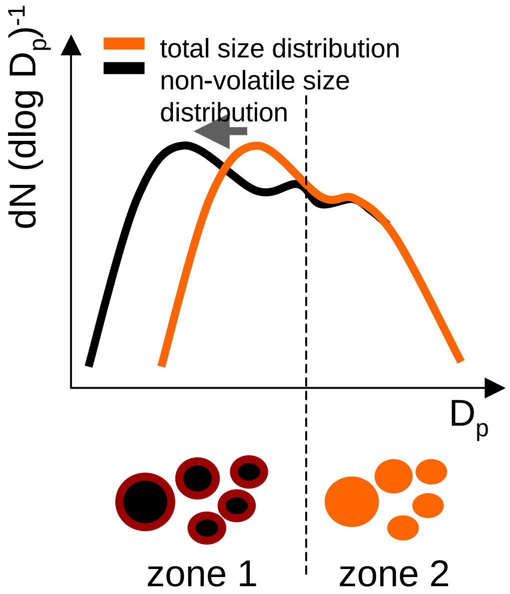

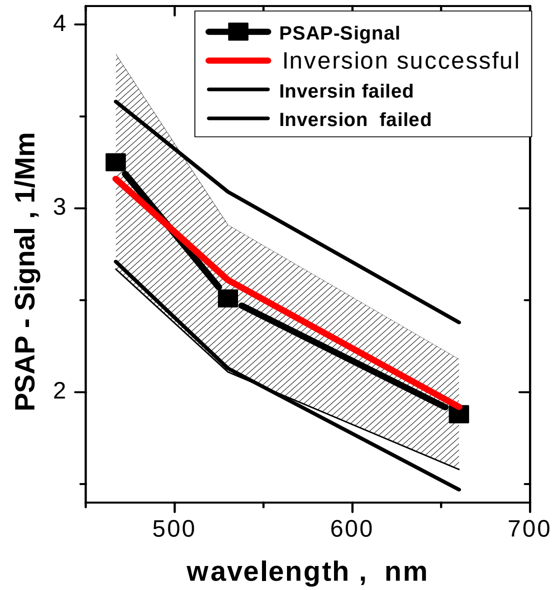

size distribution (for aerosol < 2.5 µm)

particle volatility

λ - dependence of σ_{ap} (< 2.5 µm)

Application #1: Refractive Index Determination

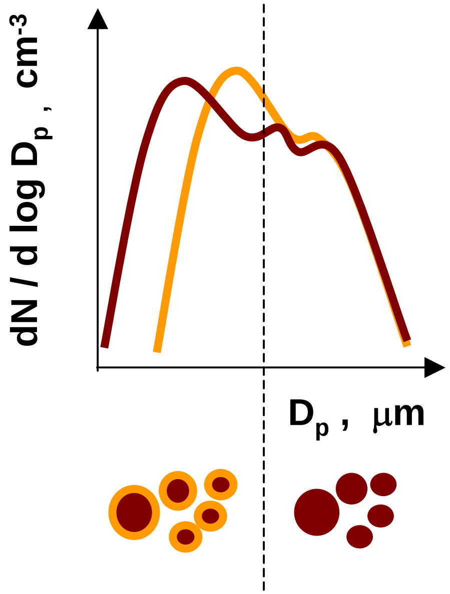

Application #1: Refractive Index Determination

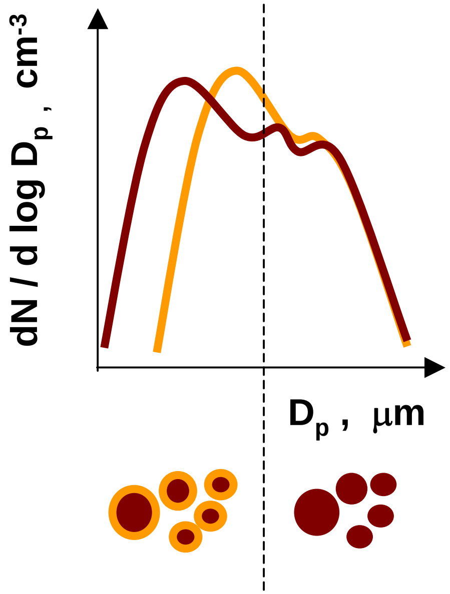

aerosol model

$$PM = \Sigma_j \, \nu_j \, C_j$$

$\Rightarrow$ refractive index

Application #1: Refractive Index Determination

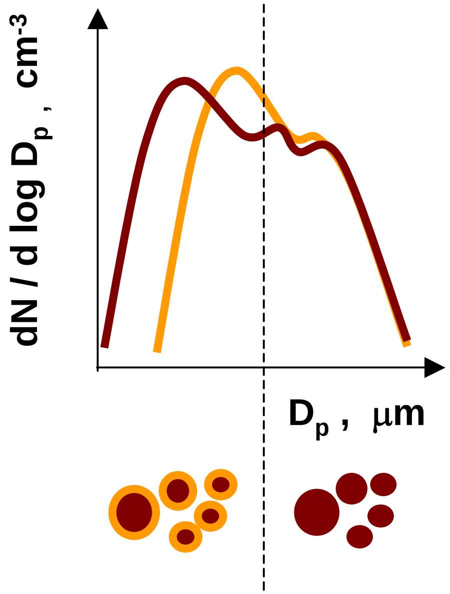

aerosol model

$$PM = \Sigma_j \nu_j C_j$$

$\Rightarrow$ refractive index

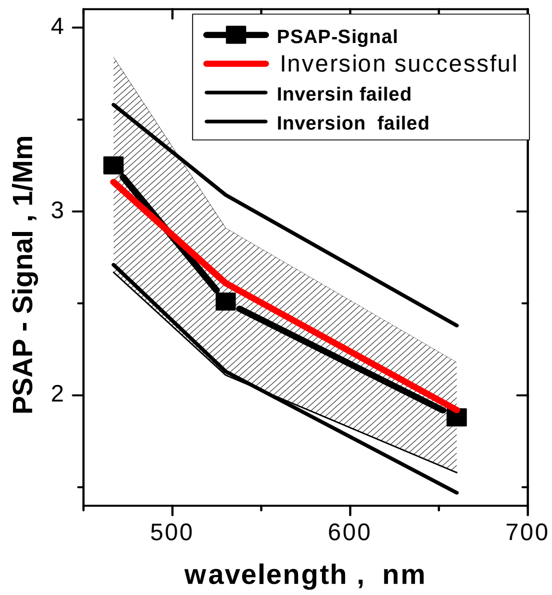

Application #1: Refractive Index Determination

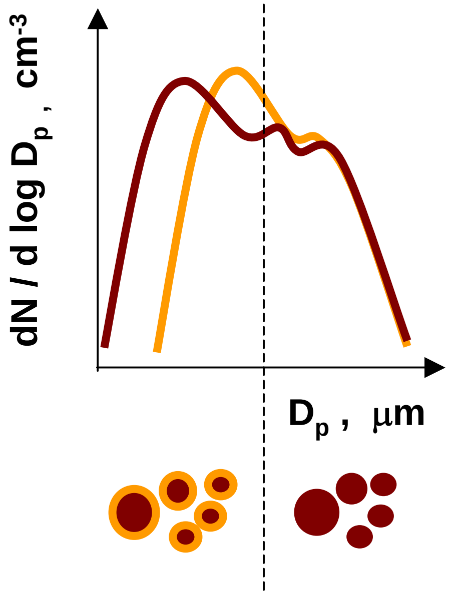

aerosol model

$$PM = \Sigma_j \nu_j C_j$$

⇒ refractive index

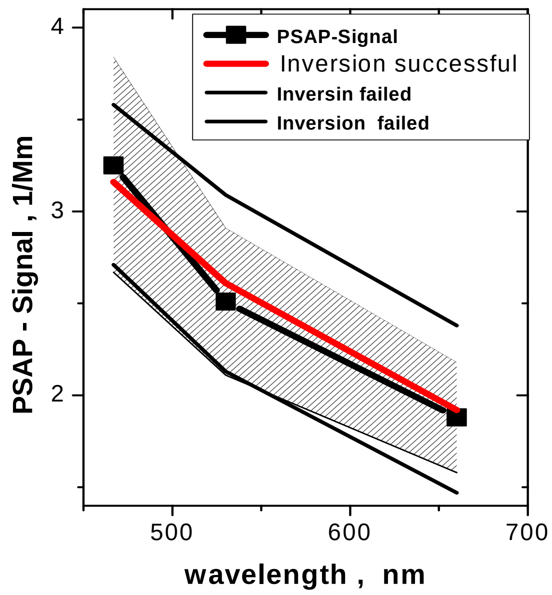

size distribution & refractive index & Mie - model ⇒ σ_{ap} , σ_{sp}

inverted absorption signal = observation ?

Application #1: Refractive Index Determination

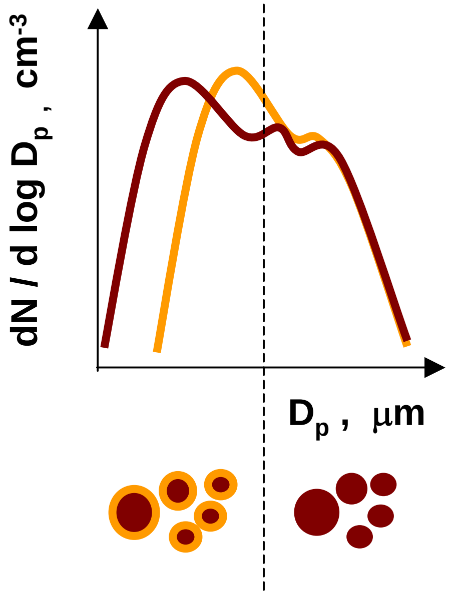

aerosol model

$$PM = \Sigma_j \, \nu_j \, C_j$$

$\Rightarrow$ refractive index

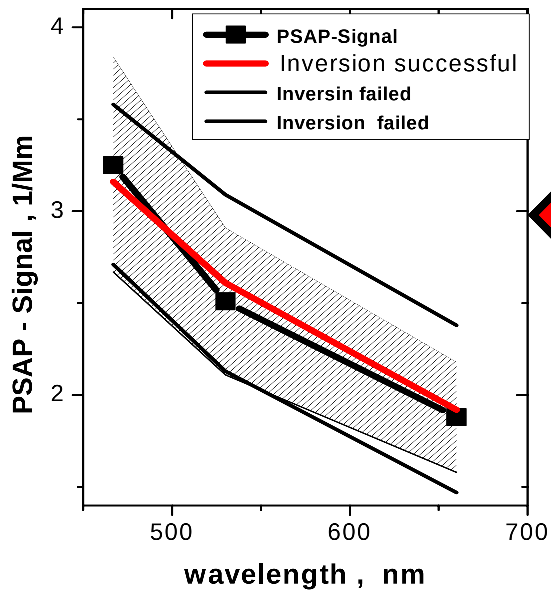

size distribution & refractive index & Mie - model $\Rightarrow$ σ_{ap} , σ_{sp}

inverted absorption signal = observation ?

NO

YES

complex refractive index , **σ_{ep} (λ) , σ_{ap} (λ) , σ_{sp} (λ) , SSA (λ)**

Application #2: Optical Closure for Dust

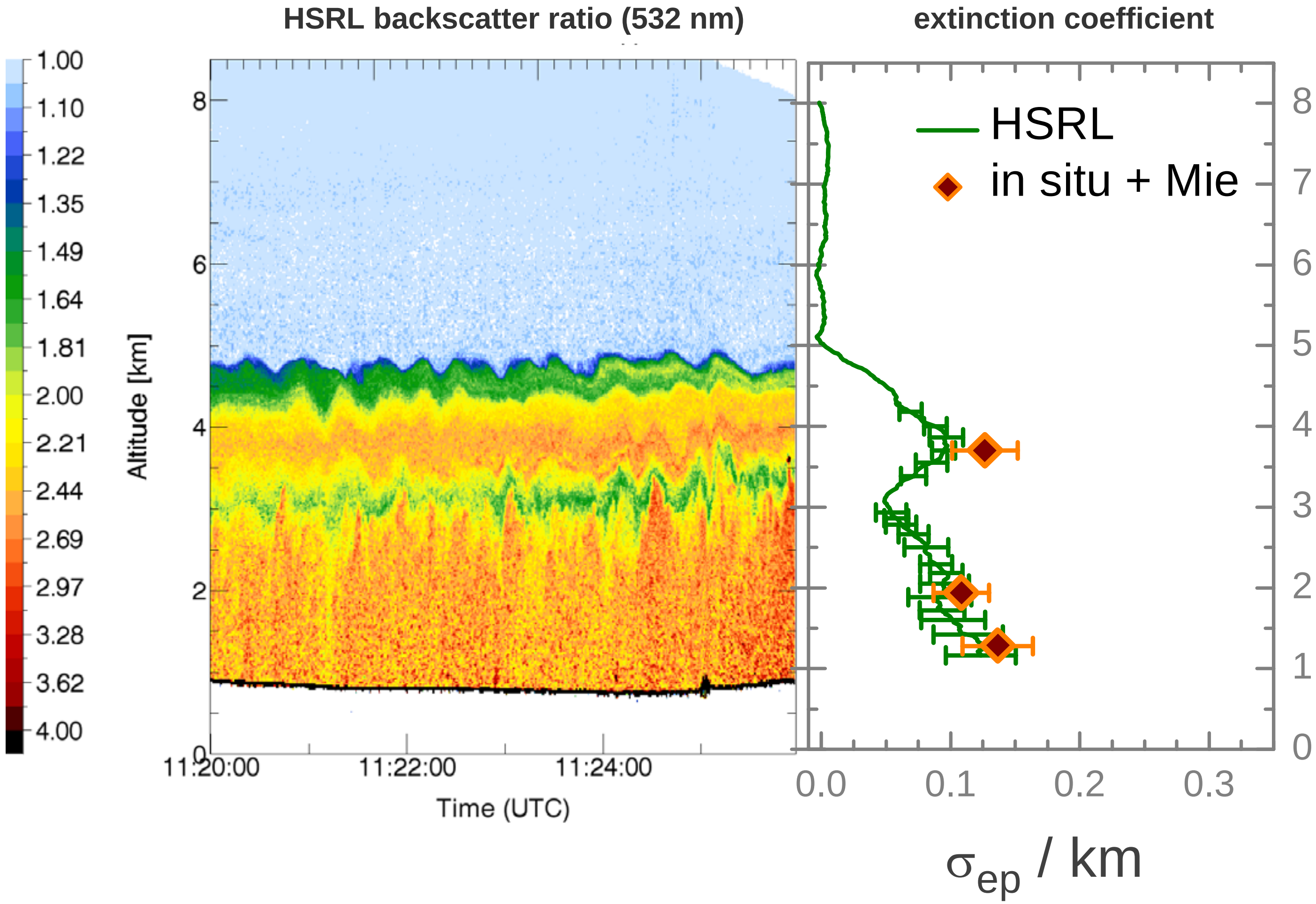

Saharan dust layer over Ouarzazate (Morocco) during SAMUM-1.

Application #2: Optical Closure for Dust

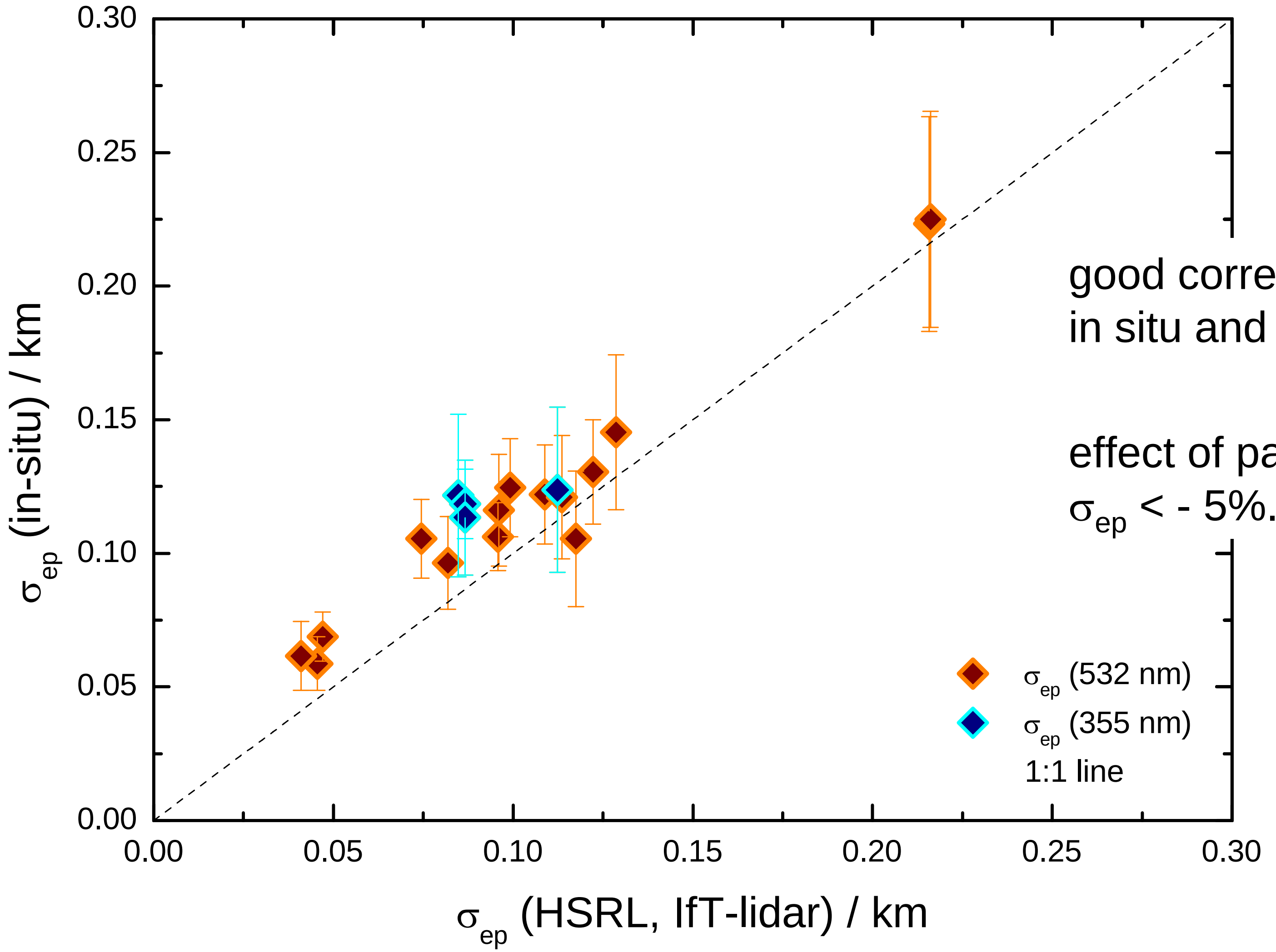

good correlation between in situ and HSRL σ_{ep}.

effect of particle shape on σ_{ep} < - 5%.

Saharan dust samples over Ouarzazate (Morocco) during SAMUM-1.

Application #2: MISR validation on 19 May 2006

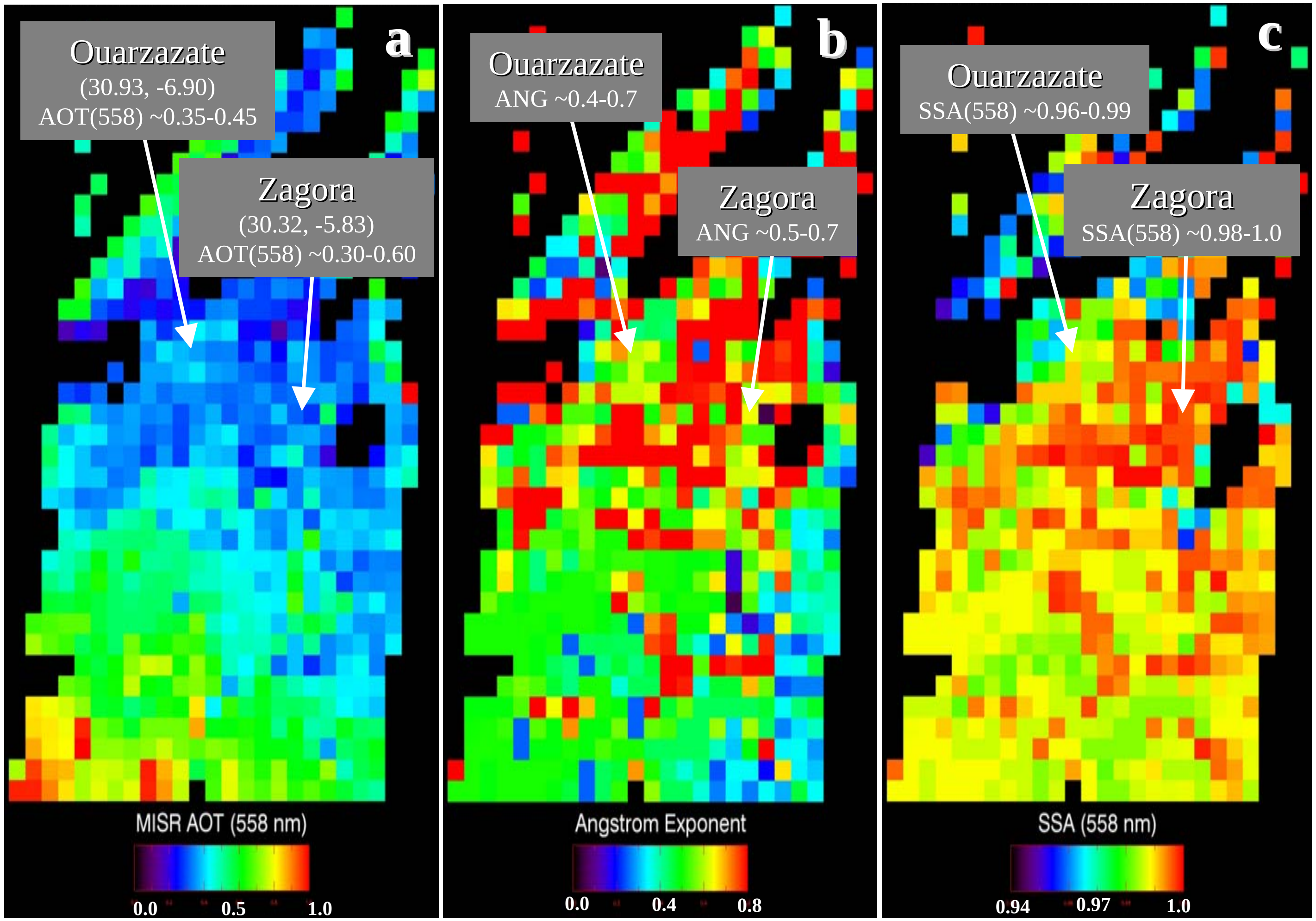

In situ data

AOT HSRL (@532)
0.38

Angström-Exp.
0.01 - 0.07

SSA
0.83 (550 nm)

Application #3: Aerosol Type Identification

Absorption Ångstroem exponent

$$\text{å}_{ap} = -[\ln(\sigma_{ap}/\sigma_{ap})] / \ln[467/660]$$

describes the wavelength-dependence of the absoprtion coefficient acc. to

$$\sigma_{ap} \propto \lambda^{-\text{å}}$$

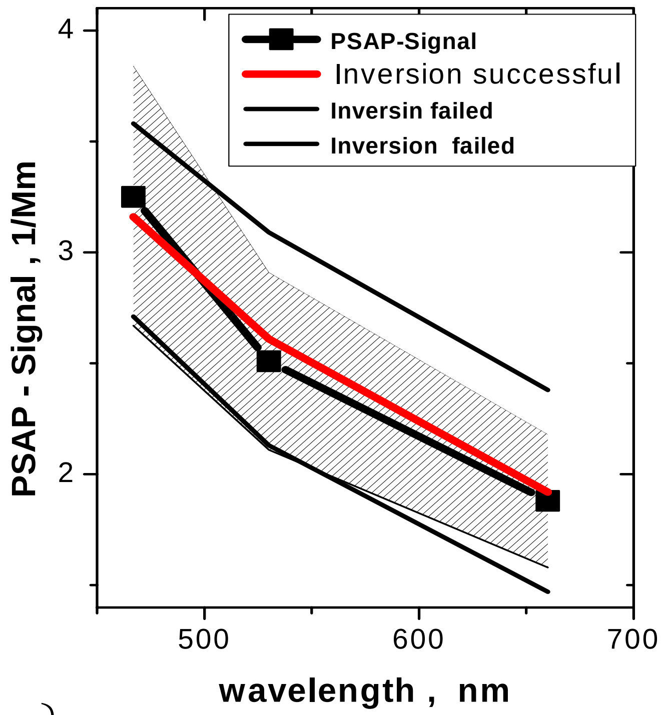

Raileigh regime $$Q_{ap}(m,\alpha) \propto \frac{D_p}{\lambda} \operatorname{Im}\left\{\frac{m^2-1}{m^2+2}\right\}$$

if the complex refractive index is almost independent of λ, as is the case for soot, then $\text{å}_{ap} \cong 1$

if the complex refractive index shows a strong λ-depence, as for dust, then $\text{å}_{ap} > 3$

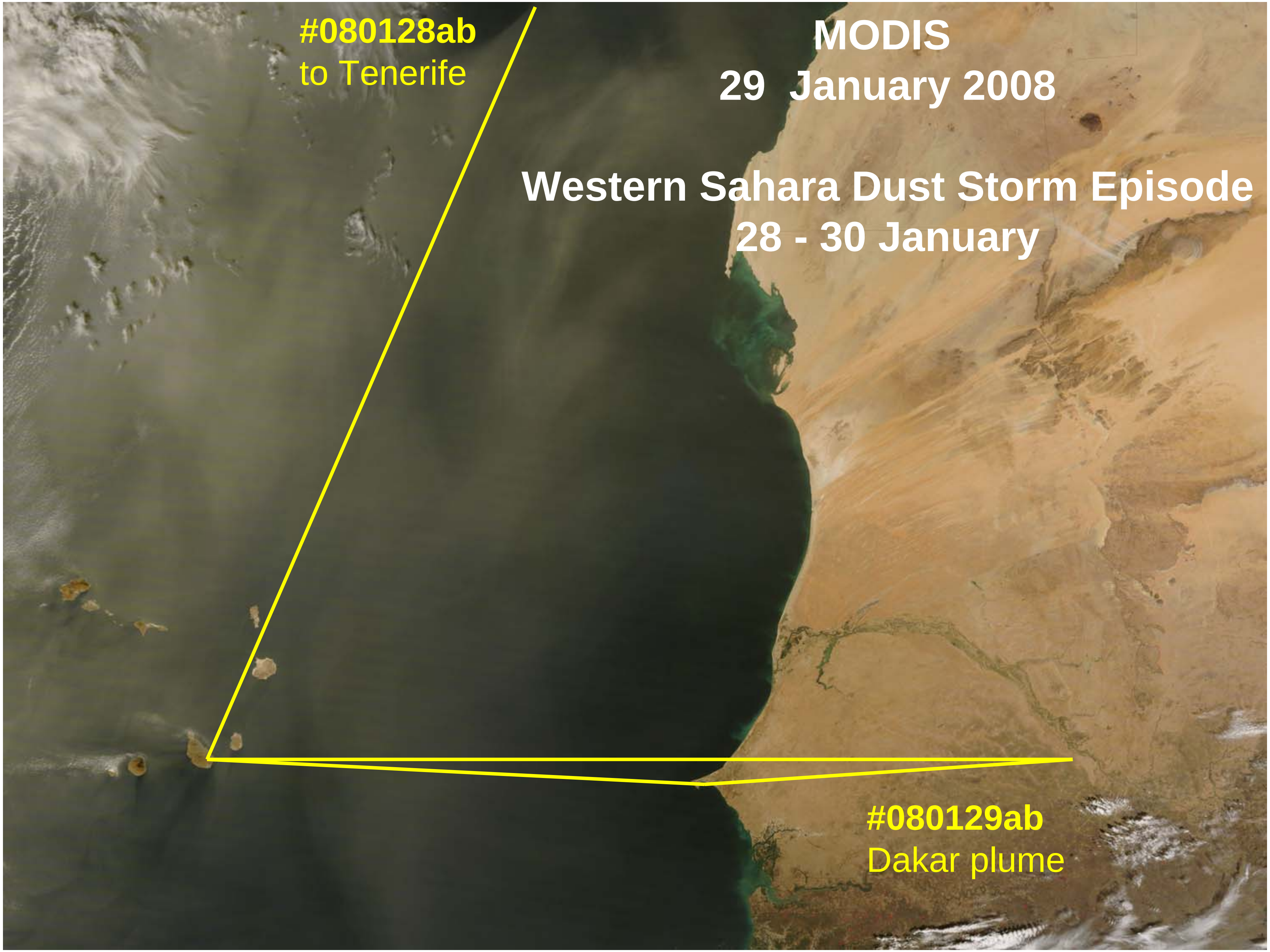
#080128ab
to Tenerife
MODIS
29 January 2008
Western Sahara Dust Storm Episode
28 - 30 January
#080129ab
Dakar plume

Application #3: Aerosol Type Identification

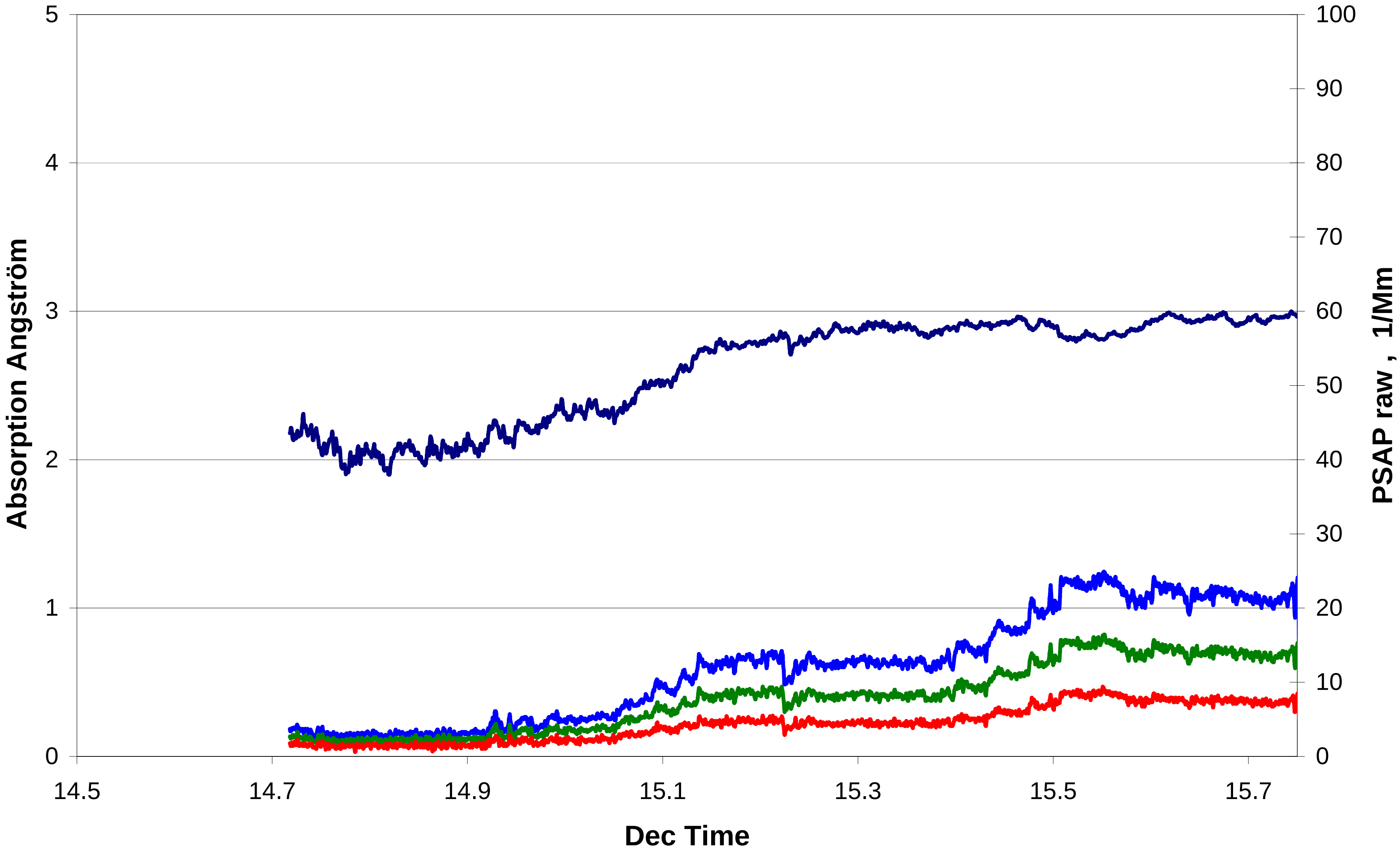

Teneriffe changing type of dust to Praia

Application #3: Aerosol Type Identification

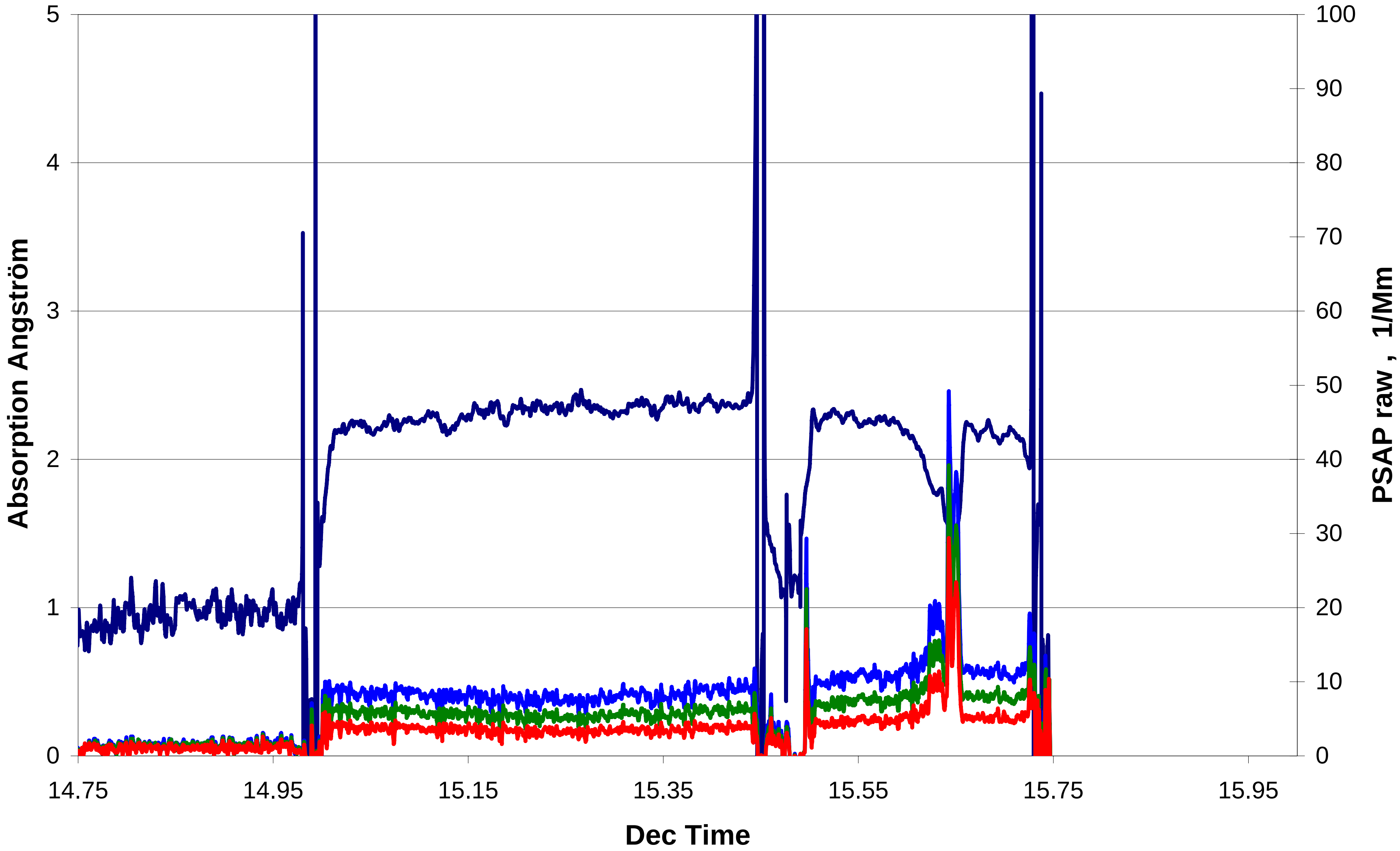

biomass burning aerosol layer

dust layer

Dakar pollution embedded in dust